



CO₂ release in simulated solutions

CCUS Innovation 2.0

Key Knowledge Deliverable 3.3



© Crown copyright 2026

This publication is licensed under the terms of the Open Government Licence v3.0 except where otherwise stated. To view this licence, visit nationalarchives.gov.uk/doc/open-government-licence/version/3 or write to the Information Policy Team, The National Archives, Kew, London TW9 4DU, or email: psi@nationalarchives.gsi.gov.uk.

Where we have identified any third-party copyright information you will need to obtain permission from the copyright holders concerned.

Any enquiries regarding this publication should be sent to us at:
nzip@energysecurity.gov.uk

Contents

Key Achievements	4
Work Package 3.1	4
Introduction	4
pH and acidity	4
Effect of CO ₂ on pH in a Ca(OH) ₂ aqueous environment	6
pH tracing experimental methodology	8
Carriers investigated: rationale	10
Release profile in simulated conditions (pH and sorption profiles)	12
Amine-impregnated silicas	12
Amine-impregnated Polymer 1-AMINE 3 carriers	17
Basic Ca(OH) ₂ testing and results – non-saturated solution	19
Conclusions and targeted optimisations based on results	21
Work Package 3.2	23
Simulated cementitious conditions optimisation – introduction	23
Carriers investigated: rationale	23
Simulated conditions testing and results – cementitious solution	25
Amine-impregnated silicas	25
Amine-grafted silicas	29
Amine-impregnated Polymer 1-AMINE 3 carriers	34
Conclusions and targeted optimisations based on results	36
Carrier optimisations based on results	38
Literature review	38
AMINE 3.1@P1	39
Amine 3.5@P1	49
Conclusions and further work	53

Key Achievements

Work Package 3.1

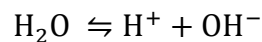
Introduction

The transfer of CO₂ to cementitious systems is governed by a series of equilibria centred around the concentration of calcium hydroxide, and therefore the basicity of cement (pH). Therefore, where certain considerations are met, the pH of a simulated cement relevant condition can be used to evaluate CO₂ release profiles.

pH and acidity

Water exists in a constant equilibrium between H₂O and its ionic products, OH⁻ and H₃O⁺. For simplicity's sake, H₃O⁺ is equivalent to H⁺ and will be herein termed as such. Where no other species present affect the equilibrium between H₂O and OH⁻ and H⁺, ionic product for water (K_w, Scheme 1) is 1.0x10⁻¹⁴ mol² dm⁻⁶ at STP.

Scheme 1: Equilibrium of water ionization and K_w.



$$K_w = [\text{H}^+ + \text{OH}^-]$$

In a neutral solution, the ionic constituents of water (H⁺ and OH⁻) are exactly equal in concentration. pH is a dimensionless measure of the quantity of H⁺ (or rather, the imbalance of H⁺ and OH⁻ in solution). Taking this neutral case as an example, a clear relationship between K_w and pH can be demonstrated:

Scheme 2: Derivation of pH from K_w

$$[\text{H}^+][\text{OH}^-] = K_w = 1 \times 10^{-14}$$

$$[\text{H}^+] = [\text{OH}^-]$$

$$\text{Thus: } [\text{H}^+]^2 = 1 \times 10^{-14}$$

$$[\text{H}^+] = 1 \times 10^{-7}$$

$$\text{pH} = -\log_{10}[\text{H}^+]$$

$$\text{pH} = 7$$

Adding an acid or base to the system disrupts the balance of H⁺ and OH⁻ in the system. A pH value change of +1 represents either a decrease in H⁺ (or increase in OH⁻) by a factor of 1000. Acids and bases act effectively H⁺ or OH⁻ donors respectively, with an important distinction

between **weak** and **strong** bases in terms of their effect on pH. What determines the strength of an acid, in principle, is the strength of its conjugate base. Where an acid HA dissociates to release H⁺ and the conjugate base A⁻, its acidity is described based on the equilibrium as follows:

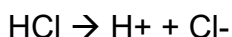
Scheme 3: Derivation of pH from Kw



A strong acid will have a weak conjugate base, pushing the equilibrium further to the right and releasing far more H⁺ in solution. Acidity and basicity are on a spectrum, however the distinction between weak and strong bases is an extremely important one for this context.

A strong acid or base is one which completely dissociates, such as hydrochloric acid (HCl) or sodium hydroxide:

Scheme 4: Dissociation of hydrochloric acid



In this case, the proton affinity (basicity) of the Cl counterion is very weak and thus the equilibrium is so far to the right it can be considered a complete reaction. Or, taking the opposing case, sodium hydroxide (NaOH):

Scheme 5: Dissociation of sodium hydroxide



Again, the equilibrium is so far too the right that every mole of NaOH added produces one mole of OH⁻. The importance of this comes when we consider this effect on pH. Recalling the equation in Scheme 2, the pH of a system containing only strong acids or strong bases can be calculated as follows:

Scheme 6: Calculations of pH in strongly acidic (top) or strongly basic (bottom) solutions

$$pH = -\log[H^+]$$

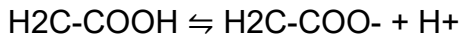
$$pH = -\log[OH^-] + 14$$

For HCl and NaOH, the equimolar generation of H⁺ and OH⁻ respectively allows direct calculation of the pH of a solution from the concentration of the respective acid or alkali. Indeed, when combining strong acids and bases, from these equations alone it is possible to calculate the endpoint pH and molar quantities required to neutralise solutions. This is particularly important as Kw is dependent on **temperature**.

An important note is that alkali earth hydroxides such as calcium are divalent, and as such release 2 moles of OH⁻ per mole of calcium hydroxide (Ca(OH)₂), also seen for some acids.

A weak acid does **not** completely dissociate. For example, adding acetic acid to water produces the equilibrium as written below:

Scheme 7: Equilibrium of acetic acid dissociation in water



In this case as there is incomplete dissociation. The equilibrium position is not completely over to the right; its position depends on the pH of the surrounding medium. Its equilibrium position at STP is defined as a pKa value, a logarithm of the dissociation constant in Scheme X, used for easier referencing over the equilibrium constant. pKa is essentially a measure of the strength of an acid, i.e. the propensity of HA to dissociate to A⁻ and H⁺. The lower it is, the stronger the acid.

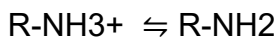
For a pure solution of a weak acid, the resulting pH can be described by the Henderson-Hasselbach equation (Scheme 8).

Scheme 8: Henderson Hasselbach equation.

$$\text{pH} = \text{pKa} + \text{Log}_{10}\left[\frac{\text{A}^-}{\text{HA}}\right]$$

When discussing weak bases, they are typically described as their respective conjugate acids. For example, amines are weak bases in solution and their pKas are best described by their ammonium conjugate acid species (Scheme 9).

Scheme 9: Amine conjugate acid deprotonation equilibria.

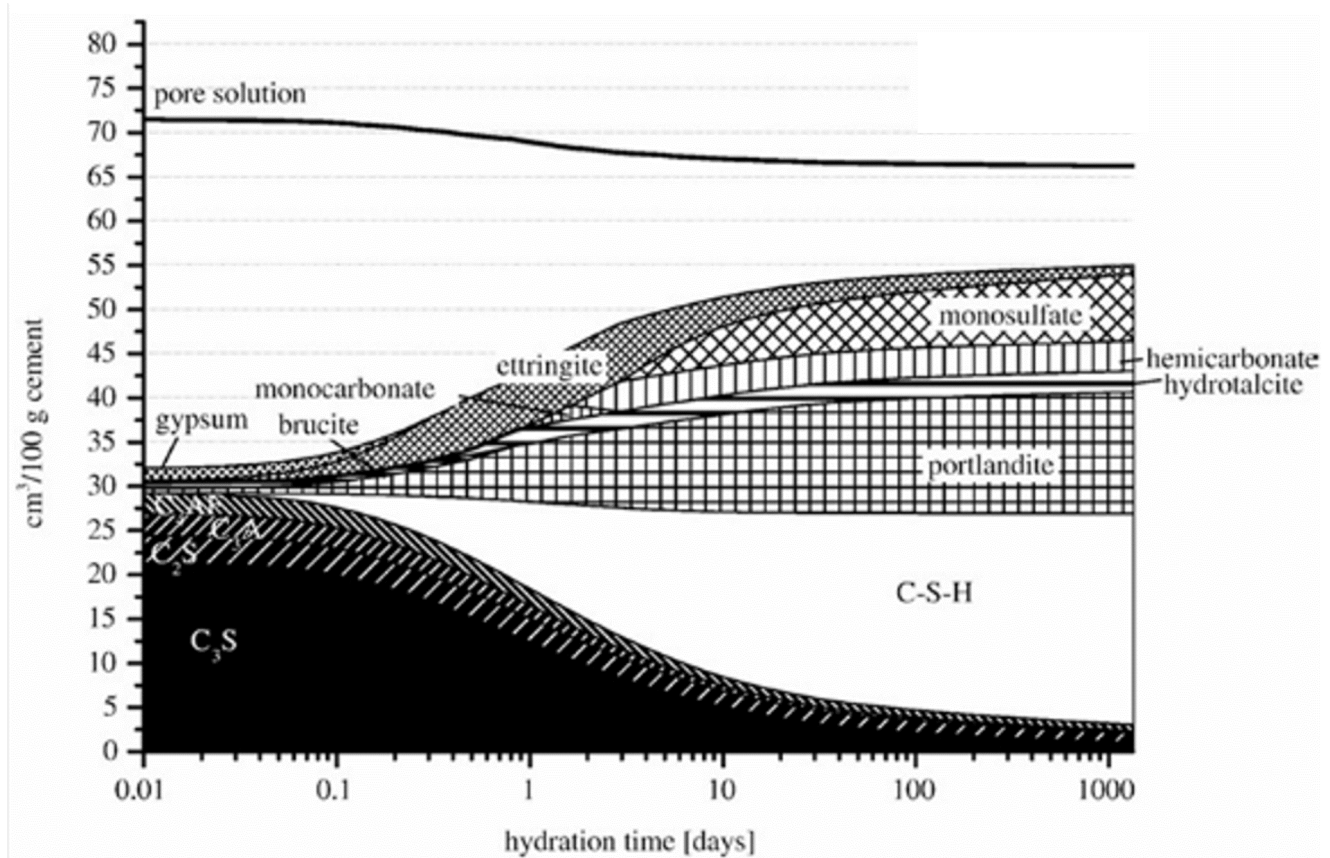


The ammonium species typically have a pH of between 9 and 10.

In essence, as weak bases and acids contribution to pH controlled systems is proportional to the pKa scaling factor, their influence on endpoint pH is typically much weaker than the concentration of strong base in solution.

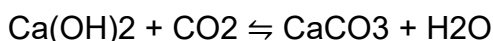
Effect of CO2 on pH in a Ca(OH)2 aqueous environment

The key basic species in cement is portlandite (Ca(OH)2), present at varying concentrations over the course of cement hydration. Portlandite is produced over the course of cement hydration as a byproduct of C-S-H formation from C2S and C3S hydration, representing 5-6 wt.% of cement composition following 1Amine 3.4y curing. Following extensive curing over 100 days portlandite concentration levels typically reach between 12-15 wt% of the final cement material (Figure 1).

Figure 1: Cement mineral evolution over time

As the targeted sink of CO₂ within cement, Portlandite (Ca(OH)₂) reacts with CO₂ in the reaction described by Scheme 10.

Scheme 10: Equilibria between the formation of portlandite and calcite



The solubility product of Ca(OH)₂ is roughly 1000X that of calcium carbonate, meaning a significant thermodynamic driving force pushing the equilibrium of Scheme X greatly to the right, favouring the formation of a solid calcium carbonate species as a permanent sequestration method. It is this transformation that is associated with densification of cementitious materials through a pore-filling model and thus the simulated conditions were developed accordingly. As you can see from Scheme X, the reaction of CO₂ with the basic Ca(OH)₂ species in solution results in the consumption of hydroxide species. In reality, in solution Ca(OH)₂ is present as Ca²⁺ and OH⁻ ions respectively, following the reaction with CO₂, this reduces the OH⁻ concentration. As described earlier, in Scheme X, the pH of a strong base such as Ca(OH)₂ is directly proportional to the concentration of OH⁻ ions in solution. As a result, monitoring the pH of a cement simulated solution containing Ca(OH)₂ is a clear route to evaluating the degree of CO₂ release in these conditions.

The strength of the alkaline solution (in terms of OH⁻ concentration) will have a direct impact on the rate of hydrolysis of the CO₂ bound species. As the cement hydration process continually develops Ca(OH)₂ in increasing quantities, and the carrier will be introduced at the

start, it is crucial to evaluate CO₂ release as a function of pH in both high Ca(OH)₂ and low Ca(OH)₂ concentration conditions.

Early stage cement simulation

At high Ca(OH)₂ concentrations (50 mM), OH⁻ is by far in excess of the CO₂ in the system and thus all CO₂ in the system can be relied upon to react before OH⁻ is consumed. From the pH traces following CO₂ release rates we are able to get a 'worst-case' scenario of selected systems in order to help inform simulated condition optimisation steps and identify promising carriers. This system is thus more representative of CO₂ release in late age cements. Key metrics here are the final pH of the systems and time taken to reach these final pH values.

Late stage cement simulation

With the low Ca(OH)₂ concentrations (5 mM), CO₂ is in excess, guaranteeing the pH drop-off to an equilibrium condition following an initial decay of pH proportional to the CO₂ release rate in **early age cements**. Because pH varies logarithmically with OH⁻ concentration, once a critical value is reached an extremely rapid and pronounced dropoff in pH will occur at the 'total' OH⁻ consumption point. Key metrics here are the 'time to dropoff' and extrapolated curves which give a significant indication of the CO₂ release rates in early age cements.

Limitations here include the reliance of pure pH value on the quantity of other acid/base species in solution such as free amines and dissolved CO₂ species, weak bases and acids which, while much smaller than the effect of OH⁻ concentration drop, will have a significant effect on the pH. As a result, the CO₂ release profiles are representative and comparable, however in this section quantifiable CO₂ release rates are very difficult to obtain. Based on these results, however, the system was then refined in WP3.2.

pH tracing experimental methodology

The methodology employed for the evaluation of CO₂ desorption from carrier materials suspended in Ca(OH)₂ solutions was as follows. Initially, the selected carrier was loaded with CO₂ at elevated pressure and temperature in an autoclave. The carrier was weighed before addition to the autoclave, which was subsequently sealed and pressurised to 10 bar with CO₂. The pressurised autoclave was added to an oven at 70 °C, where it was heated for 18 hours. After cooling, the residual pressure from the autoclave was released, and the CO₂ loaded carrier was weighed. The difference between the unloaded and CO₂ loaded mass of carrier was used to determine the adsorption capacity. From knowing carrier CO₂ capacity, the desired quantity of CO₂ could be added to simulated Ca(OH)₂ solutions to evaluate CO₂ desorption kinetics. A Ca(OH)₂ solution of a specific concentration was prepared in a centrifuge tube, the loaded carrier material was added, and the reaction mixture was immediately sealed with a pH monitoring probe suspended in the solution. A typical pH monitoring experiment set-up is shown in Figure 2, and the pH meter is shown in Figure 3.

Figure 2: pH Monitoring experimental set-up

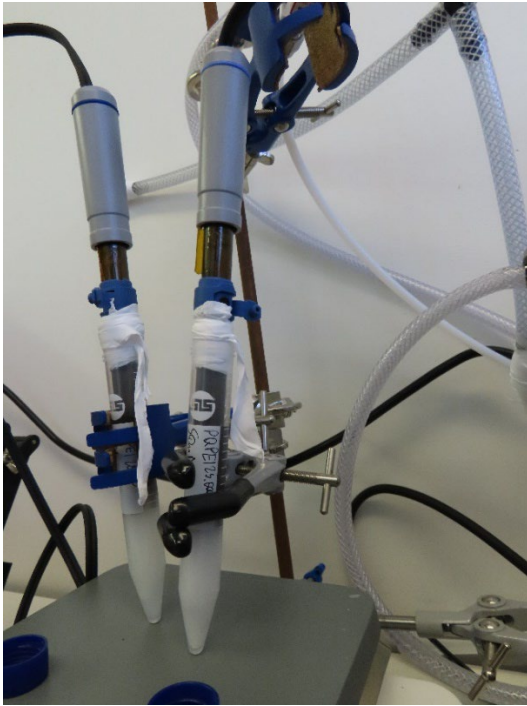
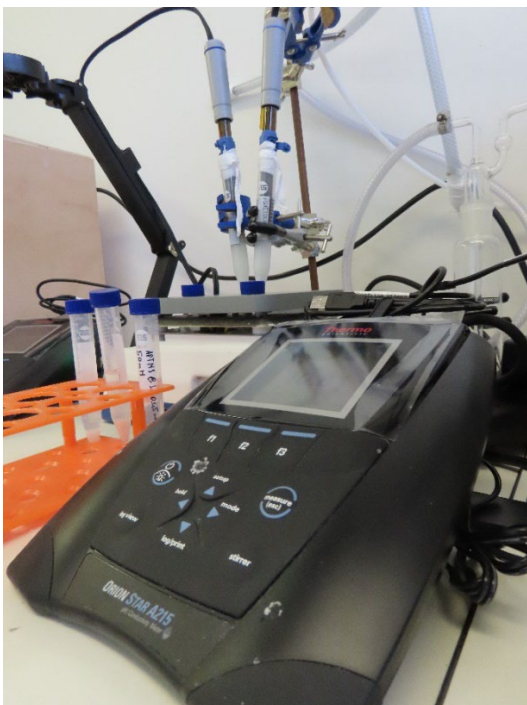


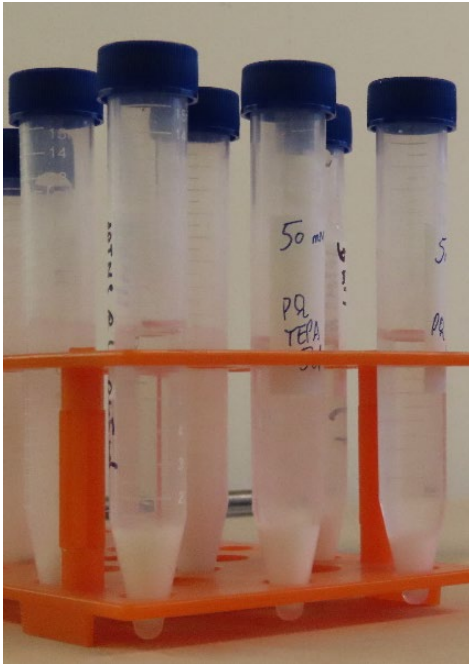
Figure 3: pH meter



Significant steps were taken to ensure the maximum possible accuracy of these experiments, including temperature control. The pH values of identical solutions vary depending on the temperature, hence these reactions were conducted in a strictly air conditioned lab, to minimise temperature fluctuations that would lead to anomalous results. However, there were still possibilities of temperature fluctuation leading to minor variations in results. The simulated solution CO₂ release experiments were also conducted in tightly sealed vessels, to prevent the dissolution of CO₂ from air into the simulated solution. While it is a slow process, CO₂ can dissolve into aqueous solutions from air, potentially adding extra CO₂ to the simulated solution

that could be wrongly attributed to CO₂ released from carrier material. Hence these reactions were tightly sealed to prevent the dissolution of CO₂ from air into the reaction mixture. The reactions were stirred, and pH measurements of the simulated solution were recorded every 2 minutes. Examples of simulated solutions with carrier material after stirring are shown in Figure 4.

Figure 4: Carrier materials after CO₂ desorption in Ca(OH)₂ solutions



Carriers investigated: rationale

Prior investigation into carrier optimisation conducted in Work Package 2 ('Carrier optimisation for the mineralisation of CO₂ in concrete') had highlighted a set of carrier materials with high CO₂ adsorption capacities, combined with slow desorption kinetics under a N₂ atmosphere. As these carriers fit the requirements for the use case of C4C, they were chosen as targets for the investigation of CO₂ desorption under highly basic conditions.

Amine impregnated silicas showed the highest CO₂ adsorption capacities of all tested materials (above 20 wt% under high pressure loading conditions at elevated temperature), while also demonstrating slow desorption rates that fall in the required time-frame for further investigation by C4C. **AMINE 1@PQ-Si** and **AMINE 2@PQ-Si** were high capacity carriers, hence one of each of these class of materials were examined for CO₂ desorption under saturated solution hydroxide solution conditions.

Amine-grafted silicas also were shown to be a viable class of carrier to fit the C4C use case, with high CO₂ adsorption capacities for AMINE 3.1 and Amine 3.5 grafted materials. Adsorption capacity and CO₂ release could also be finely tuned through simple variations in synthetic conditions, with further scope for further optimisations to this class of carrier in the

future. Hence, in addition to amine-impregnated silicas, analogues of amine grafted silicas were also chosen for simulated solution. In Work Package 2, AMINE 3.1@Si analogues prepared with different quantities of water in the synthesis demonstrated different desorption kinetics. Two analogues of this class of carrier, AMINE 3.1@Si_0.35 and AMINE 3.1@Si_0.45, were initially investigated for CO2 desorption kinetics in a saturated hydroxide solution.

Another class of carrier that showed promise in Work Package 2 as a potential viable route for use in cement were Polymer 1-AMINE 3 based carriers. Amine impregnated Polymer 1-AMINE 3 carriers showed high CO2 adsorption capacities combined with slow release rates, Polymer 1-AMINE 3 carriers impregnated with a variety of amines were examined for CO2 release rates in highly basic conditions.

The full list of carriers investigated for CO2 desorption in saturated basic solutions are shown in Table 1, with CO2 adsorption capacities and retained CO2 loadings after 48 and 480 hours under nitrogen (from previous Work Packages).

This indicative time points were chosen based on feedback from concrete companies based on their application and their applications. Considering the concrete as a simplified system, the consumption of portlandite (calcium hydroxide) by the CO2 moves the equilibrium to the left, accelerating the hydration process, resulting in the accelerated curing. This is desirable for numerous application such as precast (where cast time equals costs) as well as critical applications such as roads, runways, train tracks. While a large number of applications require the standard curing periods. Hence, various conditions are evaluated to allow subsequent modification as well as categorisation in subsequent work packages with the aim of developing an array of formulations for various applications and regions when the products are being commercialised. This allows substantial technological and commercial derisking in subsequent work packages. Furthermore, the data maybe used in the future to create further automation. This can be achieved through traditional algorithmic approach as well as further optimised by training artificial intelligence (AI), reducing future R&D costs as well as time to market for formulations in line with Research Driven Design (RDD) concepts.

Table 1: Carriers screened for CO2 desorption in saturated basic solution study - with adsorption and desorption characteristics previously measured under a N2 atmosphere

Carrier	CO2 Adsorption capacity / wt%	CO2 Retained after 48 hours / %	CO2 Retained after 480 hours / %
AMINE 2(50%)@PQ-Si	11.8	94.2	92.4
AMINE 1(50%)@PQ-Si	11.86	93.6	90.3

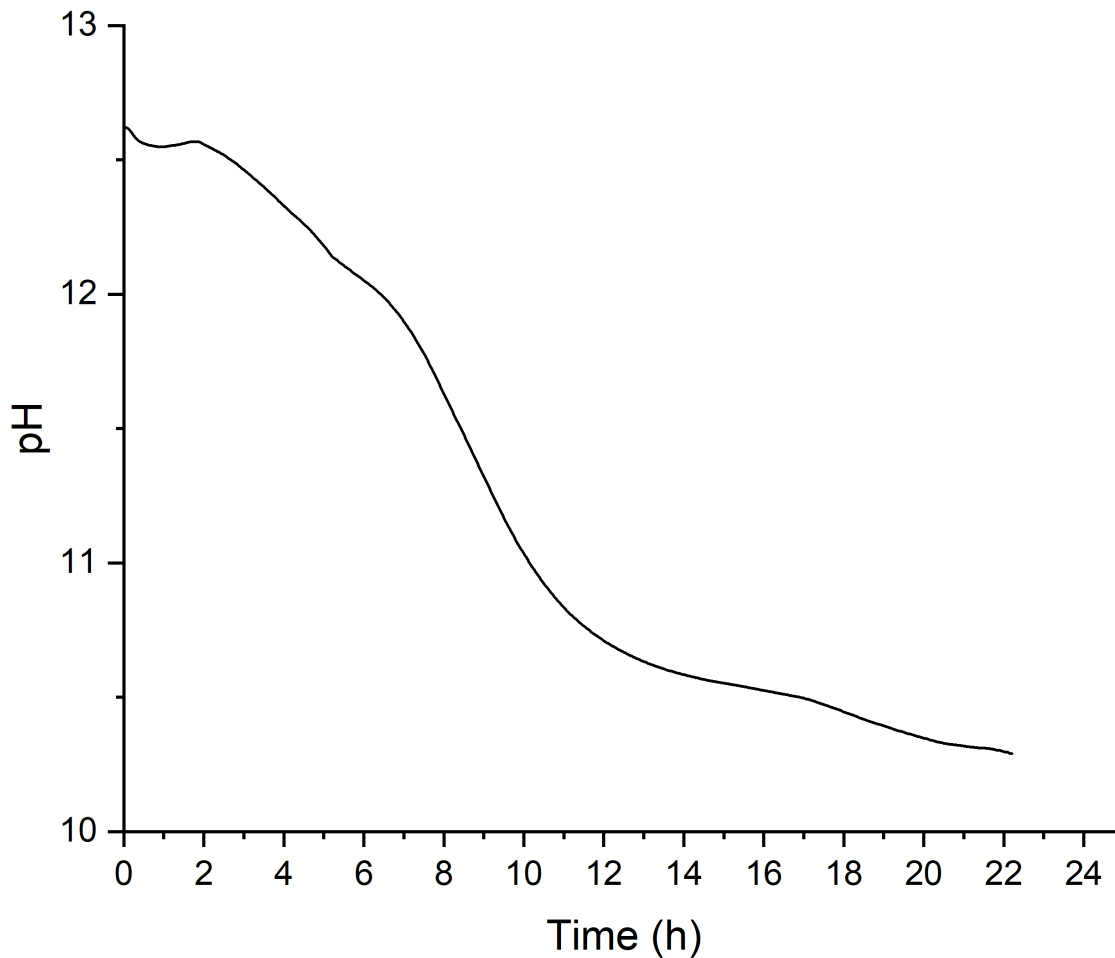
Carrier	CO2 Adsorption capacity / wt%	CO2 Retained after 48 hours / %	CO2 Retained after 480 hours / %
AMINE 3.1@Si_0.35	11.0	47.9	34.3
Amine 3.1@Si_0.45	9.15	79.0	71.6
POLYMER 1 AMINE 3-AMINE 3	22.5	- (Full desorption after 417.1 min)	-
POLYMER 1 AMINE 3Amine 3.4	14.1	- (Full desorption after 624.7 min)	-

Release profile in simulated conditions (pH and sorption profiles)

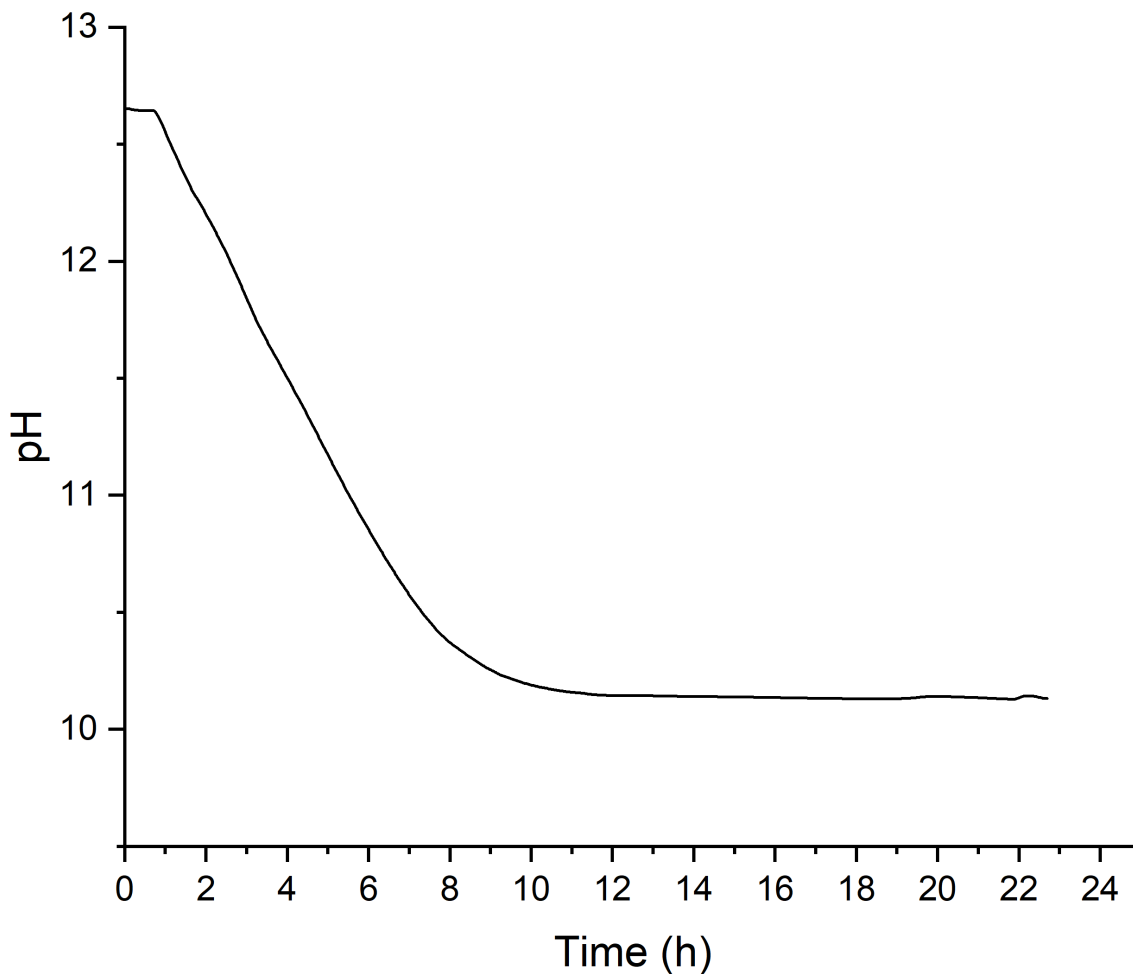
Amine-impregnated silicas

Initially, pH monitoring was conducted on a concentrated Ca(OH)₂ solution that was stirred with the addition of CO₂ loaded AMINE 2(50%)@PQ-Si. This carrier was chosen for examination as AMINE 2 represented the smallest impregnated amine that had previously been impregnated into mesoporous silica in previous Work Packages by C4C, hence the interaction of this carrier with high quantities of base was of interest. The pH evolution of the concentrated hydroxide solution with CO₂ loaded AMINE 2(50%)@PQ Si was used to determine the release profile of CO₂ from the carrier, and this is shown in Figure 5.

Figure 5: CO2 release profile from AMINE 1(50%)@PQ-Si (M25) in a saturated Ca(OH)₂ solution



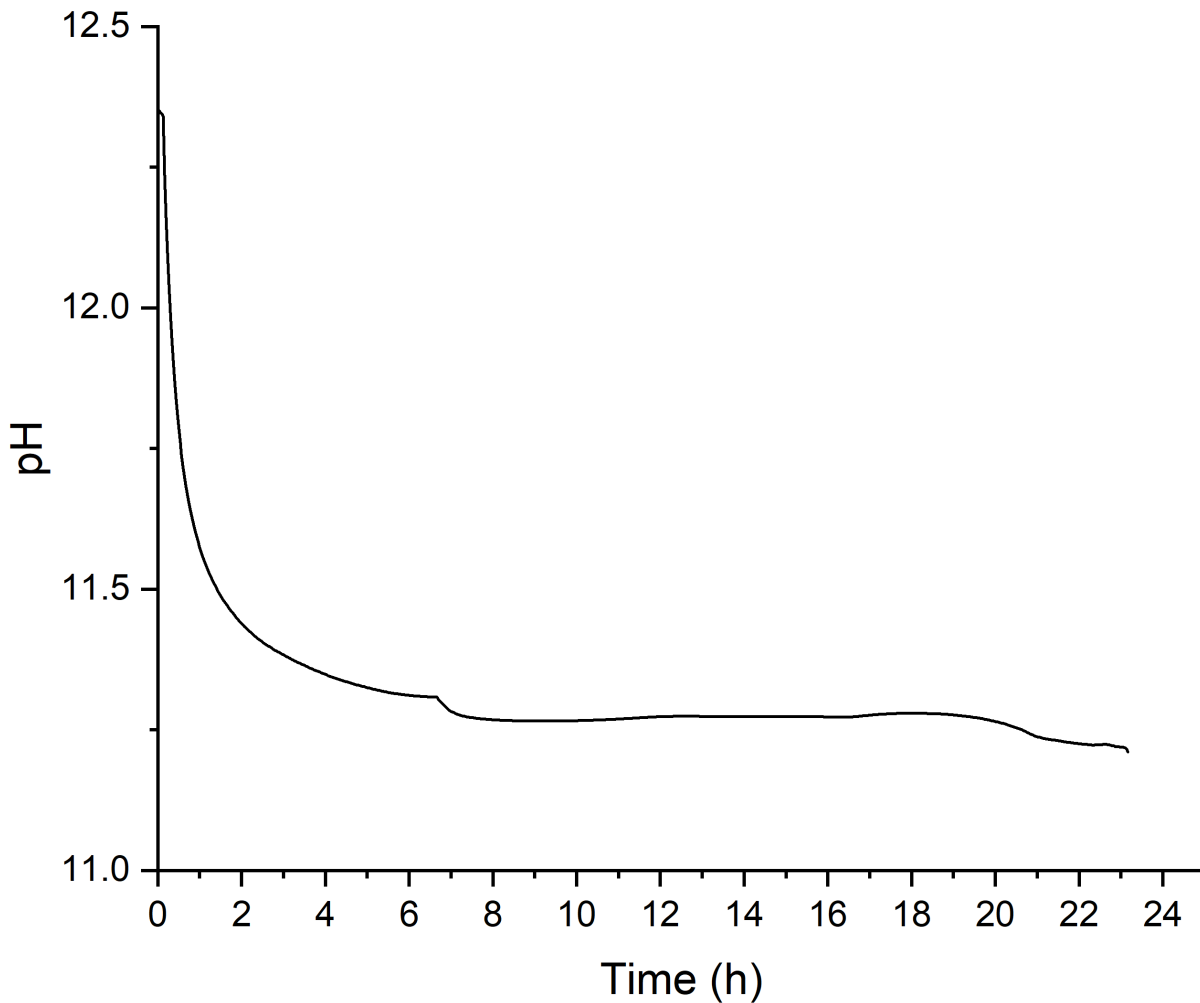
From the release profile in Figure 6, it appears that there is an induction period before the release of any adsorbed CO₂ from the AMINE 1(50%)@PQ-Si carrier material. No significant drop in pH was observed in the system until 3 hours after the CO₂ loaded carrier was added, which indicates that no desorption of CO₂ from the carrier takes place until after 3 hours. Solution pH falls at a steady rate from this point onwards during the monitoring period, where after 12 hours the rate of decrease begins to slow, indicating that CO₂ release from AMINE 1(50%)@PQ-Si initially is a moderately fast procedure, and slows as the quantity of adsorbed CO₂ decreases. The pH evolution of a concentrated Ca(OH)₂ solution with CO₂ AMINE 2(50%)@PQ-Si was also examined. AMINE 1 M25 represents the largest polymer impregnated in mesoporous silica by C4C, hence there was interest as to how CO₂ release from this carrier would differ to that from AMINE 2@PQ-Si (amine-impregnated carrier with a small impregnated amine). The CO₂ release profile AMINE 2(50%)@PQ-Si calculated from the pH evolution of the saturated Ca(OH)₂ solution bearing the carrier is shown in Figure 6.

Figure 6: CO₂ release profile from AMINE 2(50%)@PQ-Si in a saturated Ca(OH)₂ solution

Like with AMINE 1(50%)@PQ-Si (Figure 6), an induction period for the release of CO₂ from AMINE 2(50%)@PQ-Si was observed in the saturated Ca(OH)₂ solution. Interestingly, the time taken for CO₂ to start desorbing from the carrier is lower than that observed in Figure 6 for from AMINE 1(50%)@PQ-Si. The pH evolution of the concentrated simulated solution showed a moderate rate of decrease in solution pH over 10 hours, where afterwards, the constant pH of the solution suggests that total desorption of CO₂ from the AMINE 2(50%)@PQ-Si M25 had proceeded (Figure 7). Again, these results differ to those from the release profile of CO₂ from AMINE 1(50%)@PQ-Si (M25, Figure 6), where solution pH decrease takes place over a longer period of time. From these results, the large size of AMINE 1 appears to result in the slow desorption of CO₂ in hydroxide solution.

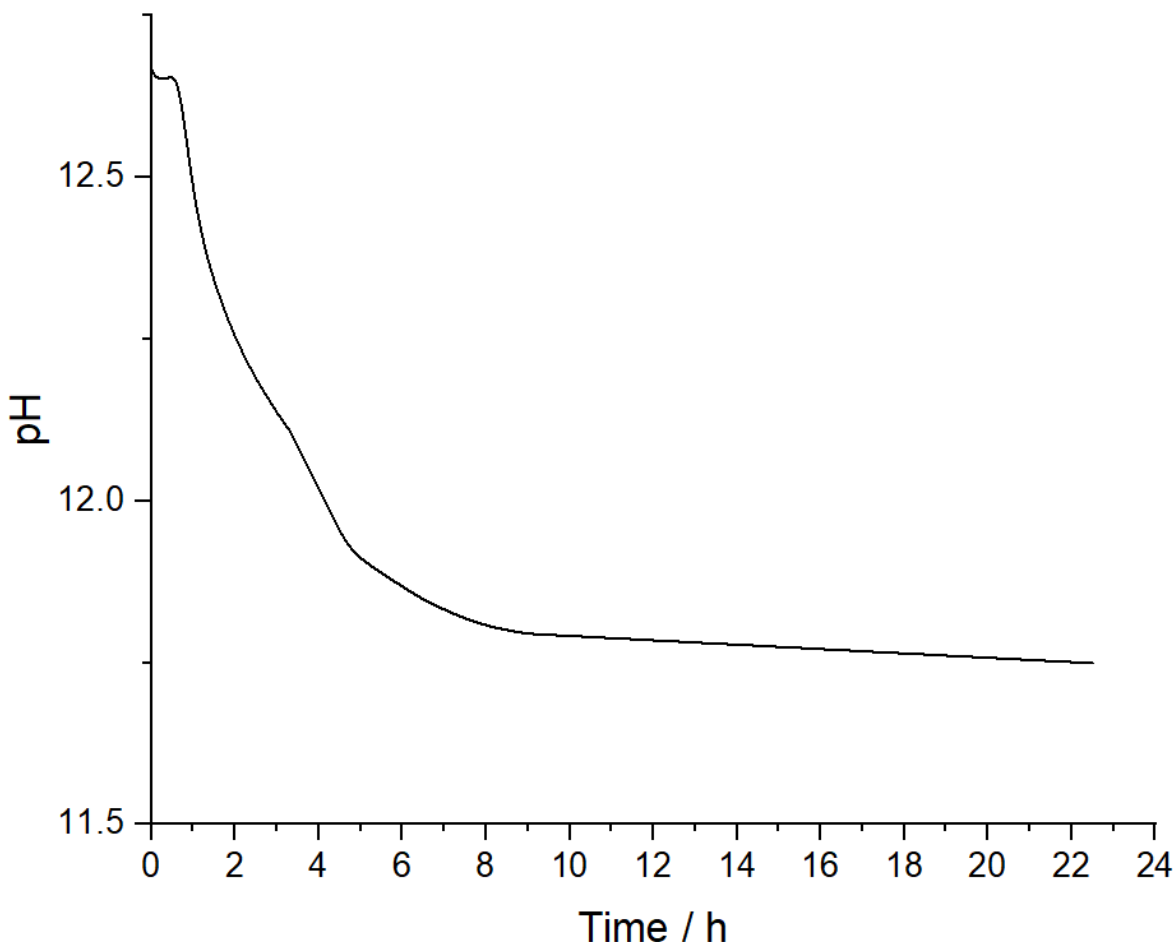
The same methodology in monitoring the pH evolution of a saturated solution of Ca(OH)₂ was applied to analyse the rate of complete CO₂ desorption from loaded amine-grafted silica carriers. AMINE 3.1@Si_{0.35} and AMINE 3.1@Si_{0.45} both showed high CO₂ adsorption capacities in Work Package 2, with significant differences in CO₂ desorption rate under a nitrogen atmosphere (Table 1), hence were ideal initial candidates to examine for CO₂ desorption rates in a saturated Ca(OH)₂ solution designed to mimic late-age cement mixtures. The CO₂ release profile from loaded AMINE 3.1@Si_{0.35} in a saturated Ca(OH)₂ solution is shown in Figure 7.

Figure 7: pH Evolution profile of a saturated Ca(OH)₂ solution prepared with the addition of CO₂ loaded AMINE 3.1@Si_{0.35}



From the release profile in Figure 7, the initial desorption of CO₂ from AMINE 3.1@Si_{0.35} can be identified as a rapid process, where the pH of the simulated solution decreases significantly over a short period of time. The rate of CO₂ release slows between 2 and 7 hours after the introduction of the CO₂ loaded carrier, where after 7 hours the pH of the solution increases gradually due most likely to temperature fluctuations. The pH evolution of a concentrated Ca(OH)₂ solution with suspended CO₂ loaded AMINE 3.1@Si_{0.45} is shown in Figure 9, a carrier that was shown in Work Package 2 to exhibit significantly slower CO₂ desorption kinetics under a nitrogen atmosphere than AMINE 3.1@Si_{0.35}.

Figure 87: pH Evolution profile of a saturated Ca(OH)₂ solution prepared with the addition of CO₂ loaded AMINE 3.1@Si_{0.45}



From the release profile presented in Figure 9, there appears to be a small induction period before the desorption of CO₂ from AMINE 3.1@Si_{0.45} proceeds. This was indicated by the stable pH of the concentrated hydroxide solution up to an hour after addition of the carrier material. When the pH of the solution does begin to fall, the initial rate of decrease is slower than that observed with the saturated solution with suspended CO₂ loaded AMINE 3.1@Si_{0.35} (Figure 7), where the point of minimum pH (and assigned point of total CO₂ desorption) occurs after 10 hours. The presence of an induction period and a slower rate CO₂ release (Figure 8) from AMINE 3.1@Si_{0.45} in a saturated Ca(OH)₂ environment compared to AMINE 3.1@Si_{0.35} (Figure 8) follows the same trend of CO₂ desorption reported in Table 1.

Interestingly, when the pH evolution curves in Figures 1 and 2 are compared with those shown in Figures 3 and 4, the total decrease in pH for the saturated hydroxide solutions with CO₂ loaded amine-impregnated silica carriers is significantly higher than the analogous systems with amine-grafted carrier materials. The quantity of CO₂ added to all of these systems were equal, hence in theory the drop in pH of these systems should be identical. These observations give an interesting insight into how amine-impregnated silicas and amine-grafted silicas are reacting in a concentrated basic environment, with regards to the leaching of amine to the solution. The decreased drop in pH observed for the solutions with CO₂ loaded amine-grafted silicas is indicative that a significant quantity of the grafted amine is being cleaved from the silica

support, then dissolving in the concentrated basic solution (as the increased pH of the end solution is indicative that dissolved basic amine is present). The lower pH of the solutions with CO₂ loaded amine-impregnated silicas (Figures 1 and 2) shows that the release of CO₂ from these carrier materials does not come as a result of the leaching of impregnated amines into the solution, and that the structure of the impregnated silica remains intact as a solid support. These are important observations that give an understanding into how different carriers will react in late-age cement conditions.

Amine-impregnated Polymer 1-AMINE 3 carriers

POLYMER 1 AMINE 3-AMINE 3 (Figure 9) and POLYMER 1 AMINE 3Amine 3.4Amine 3.4 (Figure 10) exhibited somewhat anomalous pH responses, with a high degree of fluctuation across a 24 hour time period.

This was most pronounced for POLYMER 1 AMINE 3-AMINE 3 but observed in both systems. Here, when we evaluate the overall trend of pH it appears that very little CO₂ is released over the 24-hour period, with the fluctuations likely caused by the release of the significantly basic AMINE 3 species. AMINE 3 has a pK_a in excess of 13 (i.e. the conjugate acid of AMINE 3), considerably more basic than the amine-species freed upon release of amine-based carriers. As a result, with the initial saturated solutions there is a significant degree of fluctuation. Nevertheless, these results suggest whilst this fluctuation is significant, the highly basic AMINE 3 is retaining the intramolecular structure of the respective amine carbamate and resulting in a significant degree of CO₂ retention.

Figure 98: pH Evolution profile of a saturated Ca(OH)₂ solution prepared with the addition of CO₂ loaded POLYMER 1 AMINE 3-AMINE 3

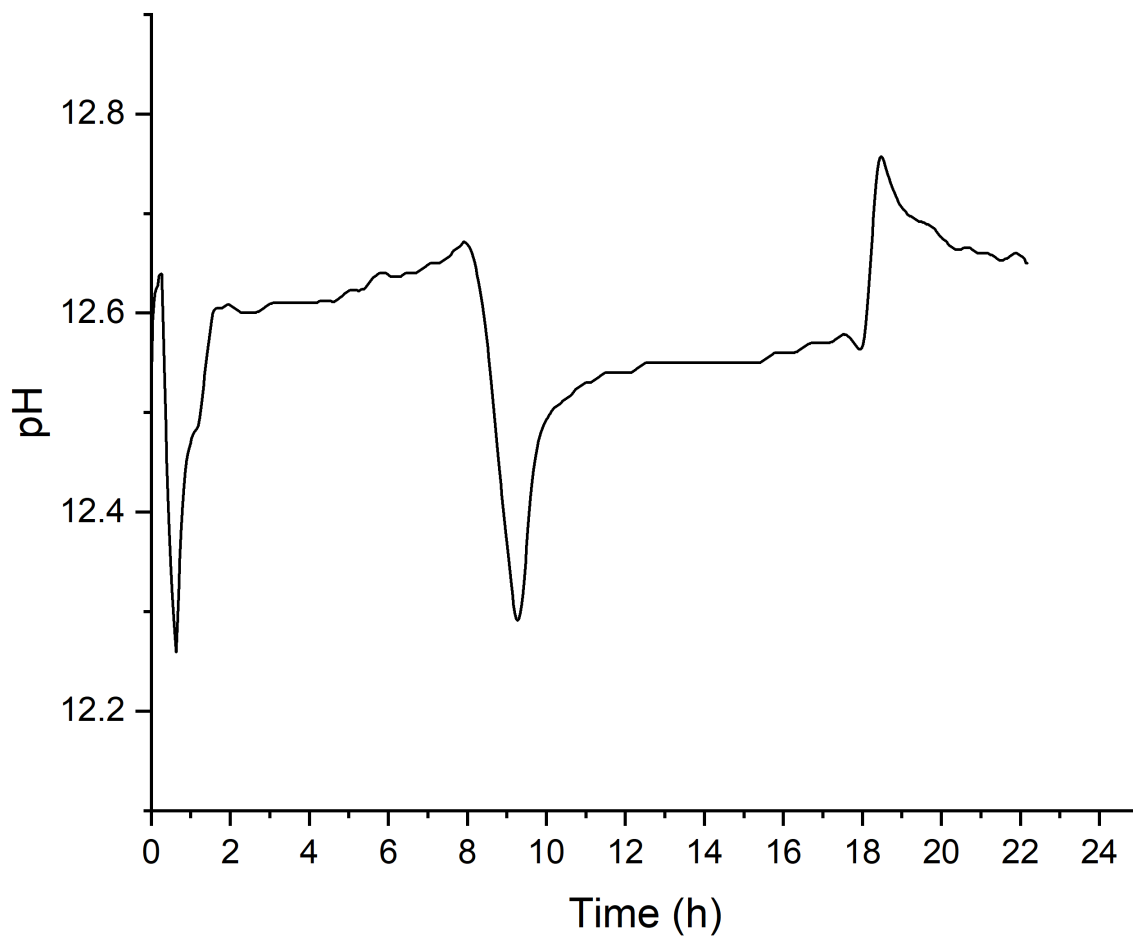
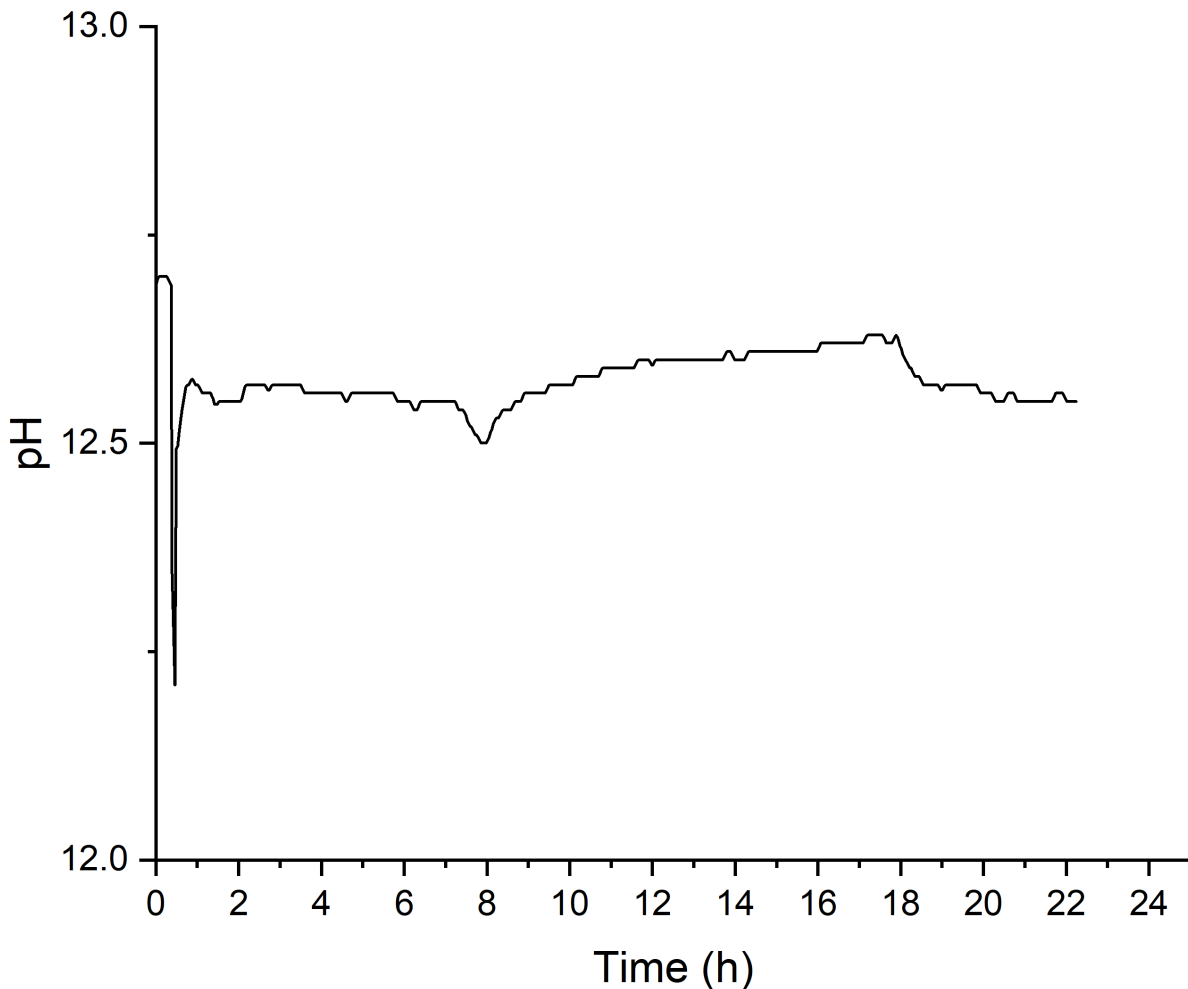


Figure 109: pH Evolution profile of a saturated Ca(OH)₂ solution prepared with the addition of CO₂ loaded POLYMER 1 AMINE 3Amine 3.4Amine 3.4



Basic Ca(OH)₂ testing and results – non-saturated solution

Experiments conducted in 3.3 gave indication as to when complete desorption of CO₂ in a saturated hydroxide solution was taking place, indicating carrier performance in a late-age cement environment. What was also of interest was how CO₂ release by carrier materials in early age cement would proceed, as portlandite development in cement would theoretically impact the rate of CO₂ desorption from C4C carrier materials. To mirror early cement environments, Ca(OH)₂ solutions of 5 mMol concentration were prepared, and CO₂ loaded carriers were stirred in these suspensions while pH was monitored. The same quantity of CO₂ was added to these systems as added to the saturated environments in the experiments detailed in 3.3, to give an indication as to whether CO₂ release rate changed in a system when CO₂ (as opposed to hydroxide) was in excess, and whether CO₂ release was purely a result of the quantity of hydroxide in the system. As the reaction of CO₂ with Ca(OH)₂ is a 1:1, reaction, through calculating hydroxide ion concentration from the monitored pH, the consumed hydroxide at a given time point in the reaction could be subtracted from the initial

quantity of CO₂ in the system to show the amount of CO₂ that had desorbed from the carrier (and reacted with Ca(OH)₂ to form CaCO₃). This would allow for a rationalisation as to whether CO₂ release was dependant exclusively on hydroxide concentration in the system, and the time at which all hydroxide ions had been consumed. This is termed as the ‘drop-off’ point. The time taken to reach this drop-off point is an indication of early stage CO₂ release and in combination with the saturated solutions gives an indication of carrier performance.

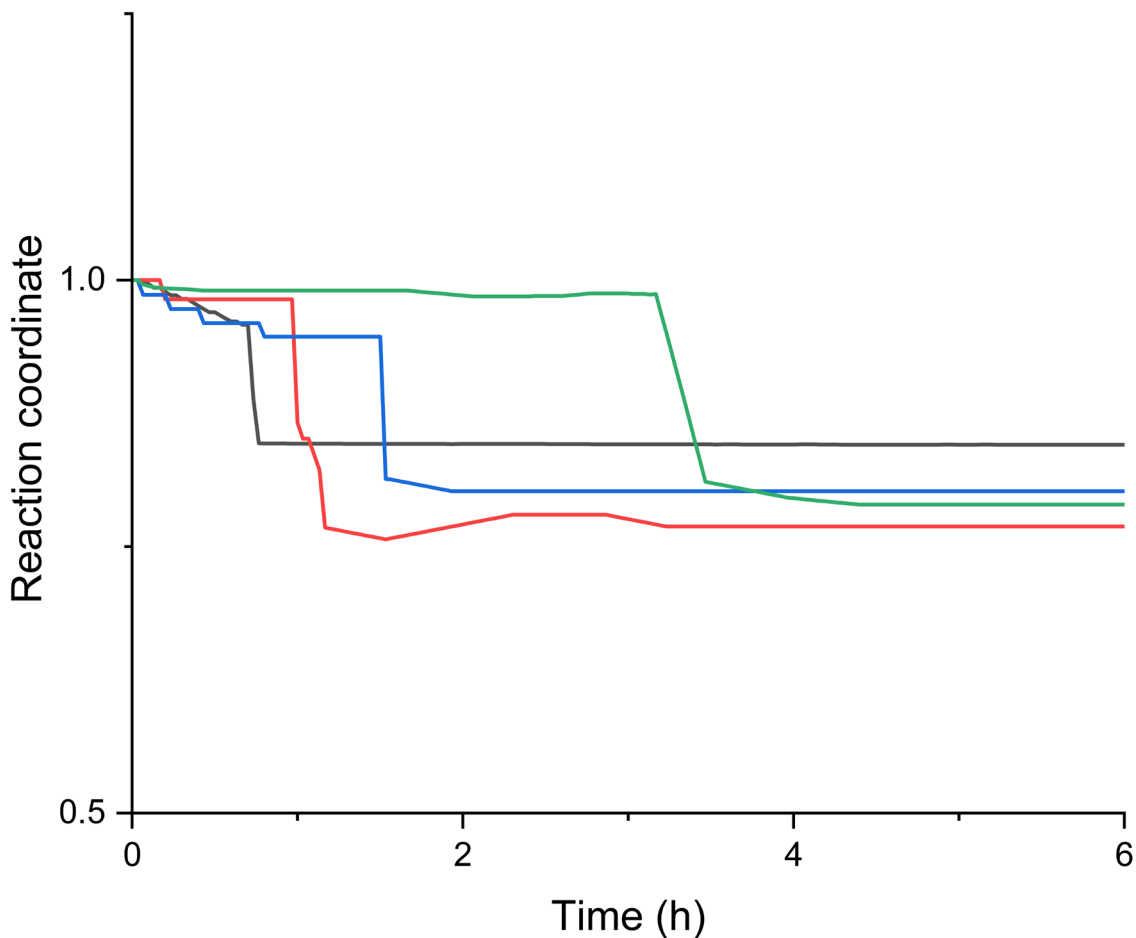
Due to the relatively low concentrations of Ca(OH)₂ solutions, these results are derived from pH values whereby the initial pH is taken as a reaction coordinate of 1, with the equilibrium values representing the total amount of CO₂ released. Small fluctuations in equilibrium values are likely due to effects of different acid/base species from the carriers and CO₂ speciation in solution. In this case, the **drop-off value is a measure of the release profile of the carrier**. Table 2 defines the ‘drop-off times’ found for the evaluated carriers, with Figure 12 demonstrating the release profiles.

Table 2: CO₂ Drop-off times of carriers evaluated in low-concentration Ca(OH)₂ solutions

Carrier	Dropoff time / h
AMINE 1(50%)@PQ-Si	3.52
AMINE 2(50%)@PQ-Si	1.20
AMINE 3.1@Si_0.35	1.87
AMINE 3.1@Si_0.45	1.52

Across the board, a very slow initial rate of CO₂ release was observed for all measured carriers, whereupon the reaction coordinate dropped to equilibrium values after 1.2-3.5 hours. It is important to note that here **not all CO₂ has been released from the carrier, as it is the OH- that is completely consumed therefore dropping the pH to a buffered value determined by CO₂ content and carrier composition**. The endpoints of the low concentration release profiles were consistent across the samples measured, with AMINE 1(50%)@PQ-si exhibiting the longest release profile by a considerable margin, reflecting the release rates in highly saturated conditions as in section 3.3.1. In all cases, release rates were considerably slower in the more dilute basic media, which suggests that in the early (1-2 day) curing times of cement.

Figure 10: pH Evolution profile of a saturated Ca(OH)₂ solution prepared with the addition of CO₂ loaded POLYMER 1 AMINE 3Amine 3.4



Conclusions and targeted optimisations based on results

Initial investigation into CO₂ release from loaded carrier materials was focused on desorption rates in environments designed to mimic late-age cement, i.e. a basic saturated solution. Through monitoring the pH of saturated Ca(OH)₂ solutions with suspended CO₂ loaded carrier materials, the time at which minimum pH occurred could be attributed to the time of complete desorption of CO₂ from the carrier. Of the amine impregnated silicas examined in this class of experiment, AMINE 1(50%)@PQ-Si (M25, Figure 6) showed slower CO₂ desorption than AMINE 2(50%)@PQ-Si (Figure 7) in strongly alkaline conditions, and a longer dropoff time in the dilute systems suggesting improved CO₂ retention by the large amine molecule. It appears from this that the nature of the amine substituent has a major effect on the accessibility of CO₂ bound species to OH⁻. As described in 3.1, pH monitoring experiments are highly sensitive, and a number of environmental factors could potentially lead to dramatic differences in for example what were assumed to be identical experiments, performed in slightly different conditions. Amine-grafted silicas were also examined for CO₂ desorption under saturated basic conditions, with differences in desorption kinetics between the two carriers trailed.

AMINE 3.1@Si_{0.45} exhibited a short induction period before a slower overall CO₂ desorption than AMINE 3.1@Si_{0.35}, which did not show any induction period before the rapid desorption of CO₂ from this carrier. While not yet known, these results indicate that there are likely significant differences in the topology of amine-grafted carriers prepared with very minor changes in water content in the respective syntheses, that attribute to different CO₂ desorption profiles in highly basic environments.

There were also some interesting differences in the nature of the pH evolution curves of the saturated basic solutions with suspended amine-impregnated and amine-grafted CO₂ loaded silica carriers. The main one being the difference in overall pH decrease in these systems. The overall pH drop in the concentrated basic solutions with amine-impregnated silicas were significantly higher than those with amine-grafted silicas, which gave an indication as to how the leaching of amines from these classes of carrier were proceeding in the highly basic solution. As amines are basic, their leaching to the hydroxide solution would theoretically result in an increase in pH, hence as the pH decrease in the simulated solutions with amine-grafted silicas is lower, then the cleaving of the covalently bound AMINE 3.1 to release the grafted amine to the system can be rationalised. The results in Figures 6 and 7 indicate that impregnated amine in AMINE 2 (50%)@PQ-Si and AMINE 1 (50%)@PQ-Si M25 is largely retained in the solid carrier, relative to the release of AMINE 3.1 grafted to silica.

Work Package 3.2

Simulated cementitious conditions optimisation – introduction

In investigation in WP-3.1, the nature of carrier CO₂ desorption in saturated basic conditions, and non-saturated basic conditions were analysed through different measurements. Through monitoring saturated solution pH evolution in highly basic conditions with suspended CO₂ loaded carrier, carrier desorption performance could be evaluated in conditions designed to mimic the harshest conditions a carrier would experience in late-aged cement (cement with high concentrations of portlandite). The results acquired from these experiments were only semi-quantifiable, as adsorbed solution hydroxide concentration was in excess of adsorbed CO₂ in the system, but the results gave a good indication of CO₂ desorption characteristics of a range of carriers in harsh cement conditions. Further experimentation on the effects of carrier addition to non-saturated Ca(OH)₂ solutions allowed for the determination of CO₂ desorption kinetics from carriers in conditions designed to mimic those found in early-age cement (with small quantities of portlandite present). Further method development allowed for quantification of the amount of CO₂ released from the respective carriers, but as CO₂ was in excess of hydroxide in these systems, the time at which hydroxide ion consumption could be rationalised, opposed to that of complete carrier CO₂ desorption.

The experiments conducted in WP-3.1 gave important qualitative information into the nature of CO₂ desorption from carriers in Ca(OH)₂ solutions representative of the conditions found in early- and late-age cement, and were built upon in WP-3.2 to gain quantitative data on the complete desorption of CO₂ in cementitious conditions. Through addition of equal quantities of hydroxide and CO₂ to a Ca(OH)₂ solution, through measuring solution pH, the concentration of hydroxide in the solution can be evaluated. As one mole of CO₂ reacts with one mole of Ca(OH)₂ to form CaCO₃, the quantity of hydroxide consumed in the system can be directly equated to the quantity of CO₂ released from the carrier material suspended in the solution. In the experiments conducted in WP-3.2, CO₂ release from loaded carriers stirred in Ca(OH)₂ solutions of 27 mM concentration were monitored, a value carefully chosen to represent the hydroxide ion concentration in 7day old cement. Through addition of a specific quantity of loaded carrier, chosen to release equal amounts of CO₂ to match the quantity of hydroxide ions into the simulated cementitious solution, CO₂ release from the carrier could be quantified through monitoring [OH⁻] consumption (measured through solution pH monitoring).

Carriers investigated: rationale

In addition to the carriers investigated in WP-3.1, additional carrier materials were investigated for CO₂ release in the simulated cementitious environment. These were chosen to gain a better understanding of how carriers with different CO₂ desorption characteristics previously analysed under a nitrogen atmosphere performed in an environment similar to cement, and

whether a correlation between CO2 desorption rates in these two systems could be determined. The range of CO2 carrier materials examined for CO2 desorption in a simulated cementitious environment are detailed in Table 3.

Table 3: Carriers screened for CO2 desorption in a simulated cementitious solution - with adsorption and desorption characteristics previously measured under a N2 atmosphere

Carrier	CO2 Adsorption capacity / wt%	CO2 Retained after 48 hours / %	CO2 Retained after 480 hours / %
AMINE 2(50%)@PQ-Si	11.8	94.2	92.4
AMINE 1(40%)@PQ-Si (AMINE 1 M25)	8.95	95.5	94.5
AMINE 1(50%)@PQ-Si (AMINE 1 M8M8)	9.63	84.3	75.0
AMINE 1(50%)@PQ-Si (AMINE 1 M25)	11.86	93.6	90.3
AMINE 3.1@Si_0.30	7.54	69.7	59.3
AMINE 3.1@Si_0.35	11.0	47.9	34.3
AMINE 3.1@Si_0.45	9.68	79.0	71.6
Amine 3.5@Si	9.50	75.6	66.6
POLYMER 1 AMINE 3-AMINE 3	22.5	- (Full desorption after 417.1 min)	-
POLYMER 1 AMINE 3-AMINE 1	17.1	64.6	52.4
POLYMER 1 AMINE 3Amine 3.4	14.1	- (Full desorption after 624.7 min)	-

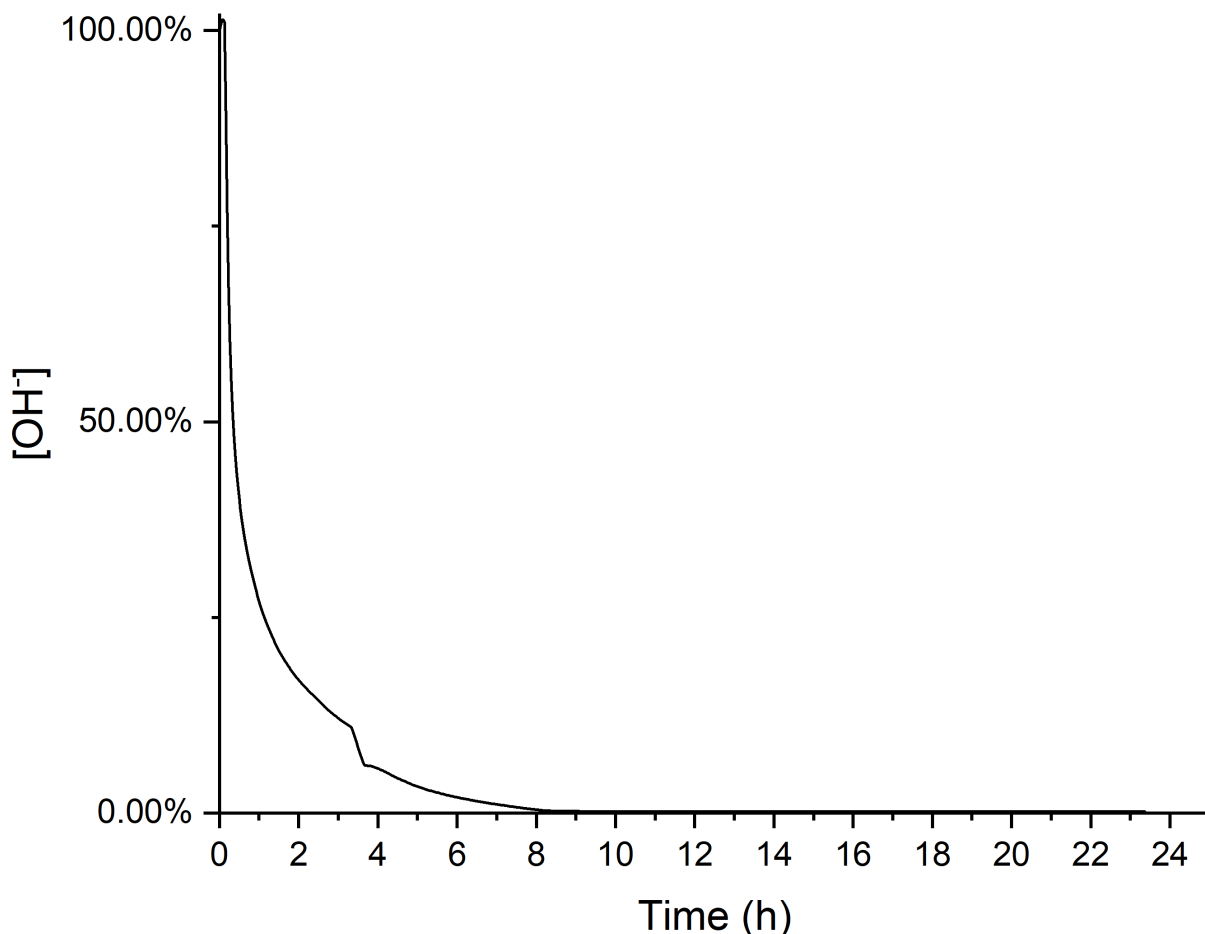
Simulated conditions testing and results – cementitious solution

From the careful design of the optimised simulated conditions, fully quantifiable results can be produced directly, as equimolar quantities of CO₂ and Ca(OH)₂ are present in solution. Whereas the saturated solutions would buffer the pH at higher ranges and the dilute systems exhibited a drop off from the complete lack of OH⁻ once fully consumed, the quantity of CO₂ remaining on the carrier here **is directly proportional to the concentration of OH⁻ ion in solution**. This is critical here as it allows a fully direct comparison of CO₂ release rates in cement simulated conditions against each other.

Amine-impregnated silicas

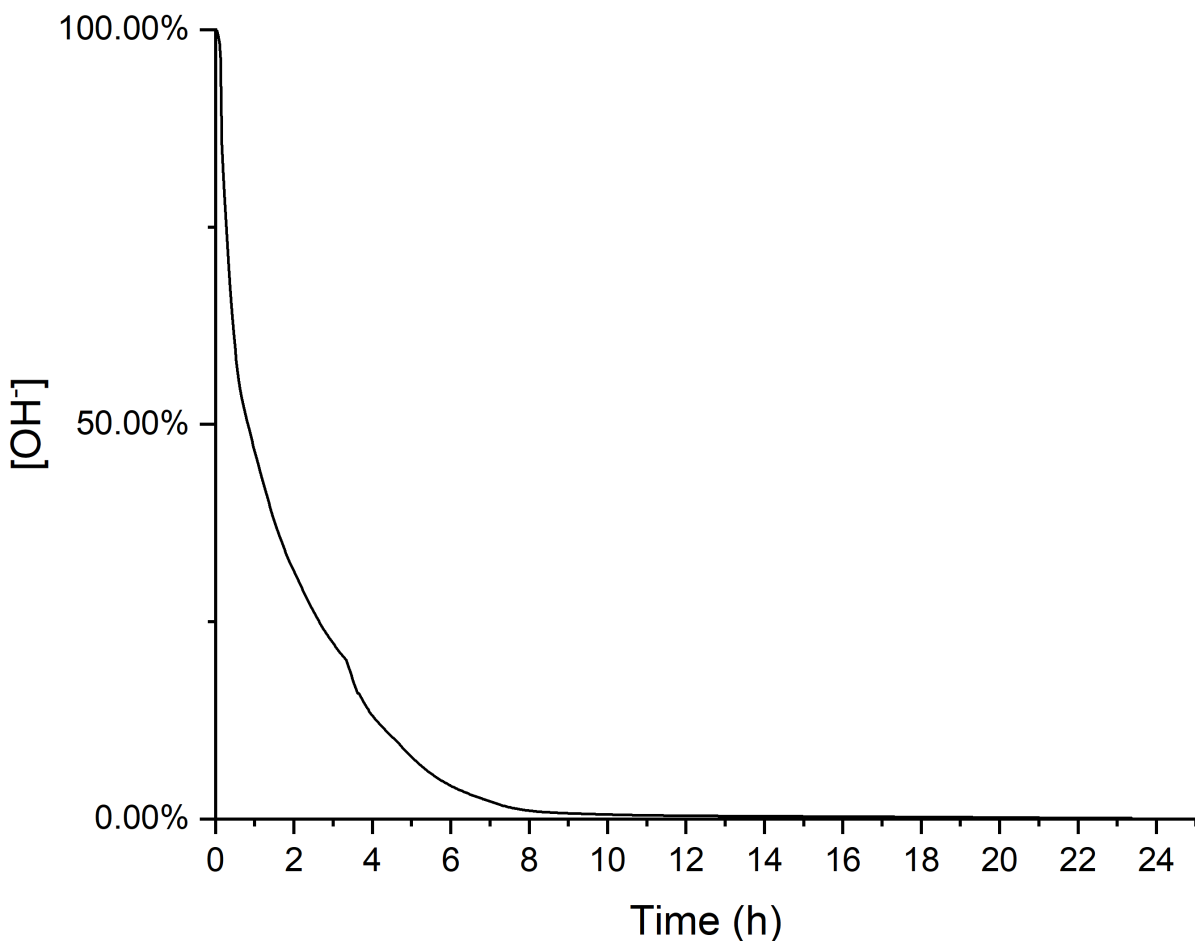
Initially, amine-impregnated silicas were examined for CO₂ desorption in cementitious solution conditions. Through monitoring pH, according to the procedure detailed in 3.1, the concentration of OH⁻ ions in simulated solutions with CO₂ loaded carrier materials could be used to rationalise the extent of release of CO₂ from the carriers. The evolution of [OH⁻] in a simulated pore solution with the addition of AMINE 1(40%)@PQ-Si is shown in Figure 14.

Figure 11: [OH⁻] Consumption profile of a simulated cementitious solution prepared with the addition of CO₂ loaded AMINE 1(40%)@PQ-Si (M8M8)



The rapid decrease of [OH⁻] in the simulated cementitious solution prepared with the addition of CO₂_AMINE 1(40%)@PQ-Si (M8M8) (Figure 14) is indicative of rapid CO₂ desorption from the carrier. As the quantity of carrier added was designed to allow for monitoring of complete desorption of CO₂ (through addition of equal quantities of Ca(OH)₂ and CO₂ to the simulated system), complete consumption of OH⁻ in the system is indicative of complete desorption of CO₂ from the carrier material. From the [OH⁻] evolution profile in Figure 14, complete desorption of CO₂ from CO₂ loaded AMINE 1(40%)@PQ-Si (M8M8) can be rationalised to take place after 8 hours in a simulated cementitious solution. The study of CO₂ desorption from AMINE 2(50%)@PQ-Si in a simulated pore solution was also conducted, and the [OH⁻] evolution curve obtained from this experiment is shown in Figure 15.

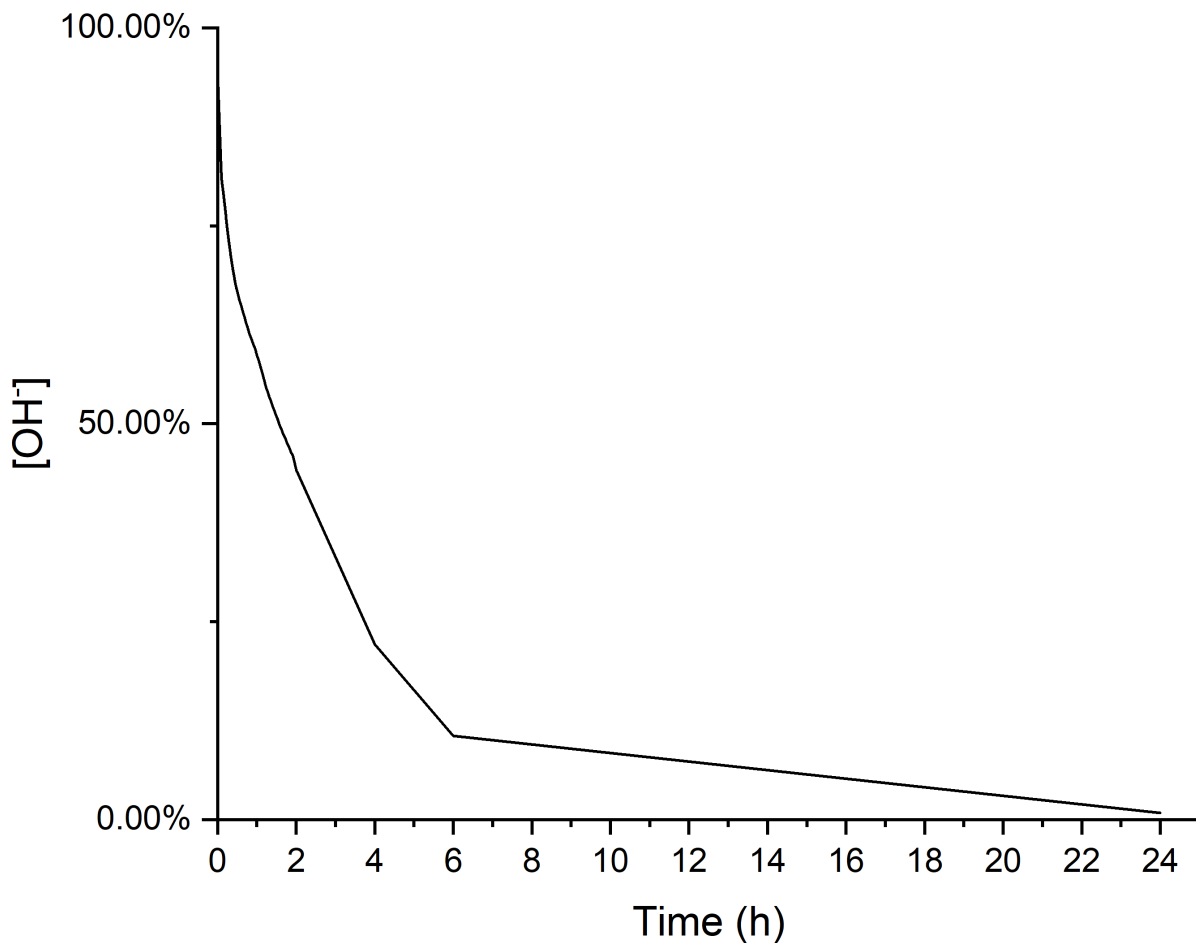
Figure 12: [OH⁻] Consumption profile of a simulated cementitious solution prepared with the addition of CO₂ loaded AMINE 2(50%)@PQ-Si



As observed with AMINE 1(40%)@PQ-Si (M8M8) (Figure 14), CO₂ desorption from CO₂_AMINE 2(50%)@PQ-Si also a facile process. A similar desorption profile is observed, over a slightly longer time period than observed with the AMINE 1(40%)@PQ-Si (M8M8), with total consumption of [OH⁻] (and complete CO₂ desorption) observed after a duration of 11 hours. Both AMINE 2 and AMINE 1 (M8) represent relatively small amines to impregnate into silica, and from the desorption results presented in Figures 14 and 15, likely do not saturate the internal volume of the impregnated mesoporous silica. This would explain the fast consumption of [OH⁻] in the system, where hydroxide ions can readily diffuse into the silica to react with the carbonated AMINE 1 and AMINE 2 to form calcium carbonate. Evidently, from

the simulated cementitious solution $[\text{OH}^-]$ evolution data presented in Figures 14 and 15, AMINE 1(40%)@PQ-Si (M8M8) and AMINE 2(50%)@PQ-Si are not viable carriers for use by C4C to promote the slow release of CO₂ into cement mixtures. The use of higher Mw AMINE 1 was predicted to promote the slower release of CO₂ by the amine-impregnated silica class of carrier, owing to a predicted increased density of pore filling to restrict access of hydroxide ions to CO₂ loaded on the impregnated amines. Initially, CO₂ desorption from AMINE 1(40%)@PQ-Si (M25M25) was examined, with the $[\text{OH}^-]$ evolution profile of this experiment detailed in Figure 16.

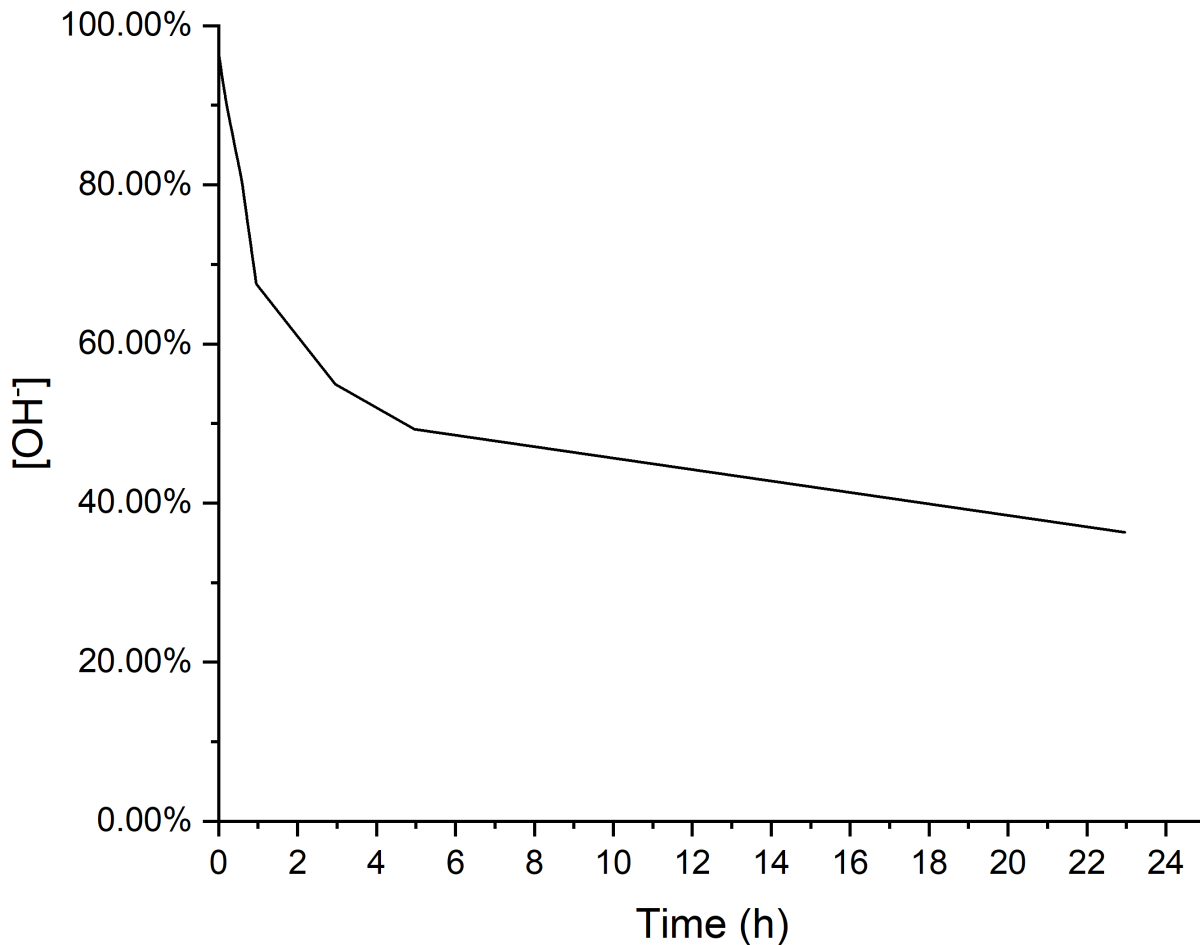
Figure 13: $[\text{OH}^-]$ Consumption profile of a simulated cementitious solution prepared with the addition of CO₂ loaded AMINE 1(40%)@PQ-Si (-M25)



Using a AMINE 1(40%)@PQ-Si prepared with a higher molecular weight polymer has a marked improvement over the smaller chained analogue regarding CO₂ desorption in a simulated cement environment. When comparing $[\text{OH}^-]$ evolution of a simulated solution with AMINE 1(40%)@PQ-Si (Mw 800) (Figure 14) and AMINE 1(40%)@PQ-Si (M25M25) (Figure 16), the solution with the M25M25 impregnated silica shows a significantly slower hydroxide consumption than that with the M8 impregnated silica. After the 24-hour measuring period, there is a fraction of $[\text{OH}^-]$ remaining (Figure 16), meaning that the carrier still has adsorbed CO₂ present, albeit a very small quantity. This highlights the increased difficulty for hydroxide ions to react with adsorbed CO₂ on the carrier, with a working hypothesis being that ion diffusion to adsorbed CO₂ is restricted by the significantly increased polymer size impregnated in the mesoporous silica. It was further predicted that increasing the loading of high Mw AMINE

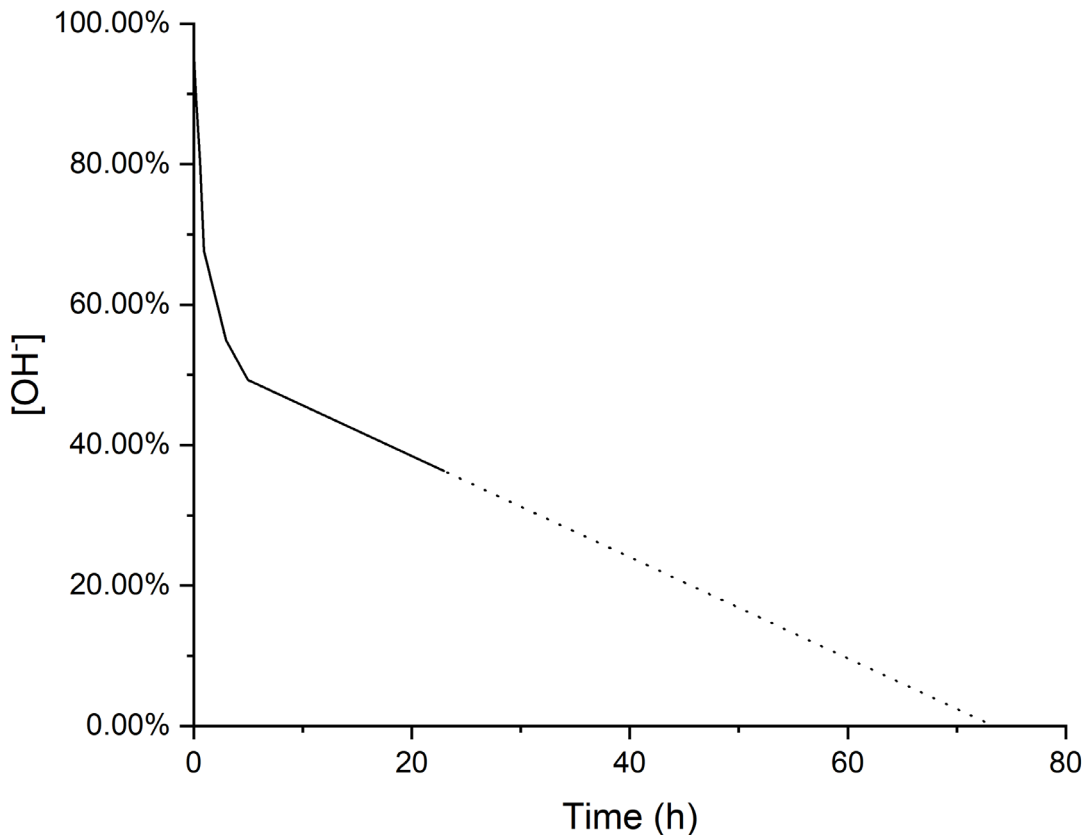
1 into the silica would further promote the slowing of CO₂ desorption in the simulated solution environment, hence CO₂ loaded AMINE 1(50%)@PQ-Si was also examined for [OH⁻] consumption in the simulated cementitious solution environment. The [OH⁻] evolution curve for this experiment is detailed in Figure 17.

Figure 14: [OH⁻] Consumption profile of a simulated cementitious solution prepared with the addition of CO₂ loaded AMINE 1(50%)@PQ-Si (M25)



Increasing the loading of high Mw AMINE 1 was conducive to slowing CO₂ desorption from impregnated carrier material. While negligible hydroxide was present after 23 hours in the simulated cementitious solution with the addition of CO₂ loaded AMINE 1(40%)@PQ-Si (M25) (Figure 16), in the analogous system with CO₂ loaded AMINE 1(50%)@PQ-Si (M25) (Figure 17), 36% of the initial concentration of hydroxide ions in solution are present after the same time period. This is a marked improvement over the analogue with the lower loading of high Mw AMINE 1, and further indicated that increasing the bulk of impregnated material is beneficial to prevent hydroxide diffusion to adsorbed CO₂ present in impregnated silica material. After 5 hours in the simulated cementitious solution, the consumption of hydroxide appears to proceed at a constant rate (Figure 17), hence this profile can be extrapolated to give an indication of the time at which complete CO₂ desorption from AMINE 1(50%)@PQ-Si (M25) proceeds under these controlled conditions. An extrapolated [OH⁻] consumption curve from the data presented in Figure 17 is detailed in Figure 18.

Figure 15: Extrapolated [OH⁻] consumption of the simulated cementitious solution prepared with the addition of CO2 loaded AMINE 1(50%)@PQ-Si (M25)

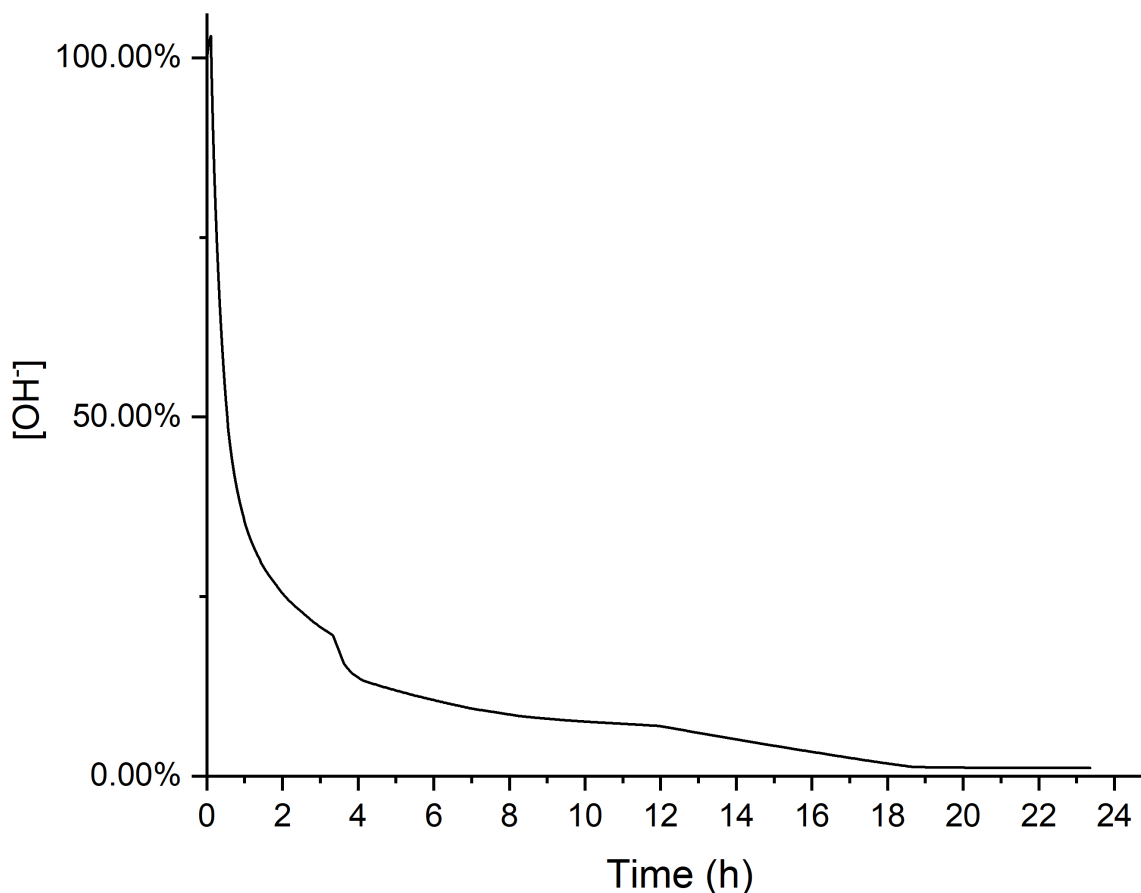


Taking the hydroxide consumption of the simulated cementitious solution with CO₂ loaded AMINE 1(50%)@PQ-Si (M25) as constant after 5 hours, from the extrapolated desorption profile in Figure 18, the time of complete CO₂ desorption from the carrier can be calculated to be 73.4 hours. After 48 hours in the simulated cementitious solution the quantity of initially adsorbed CO₂ remaining on the carrier can be projected to be 18.3 %. Of the amine-impregnated materials examined in this study, only AMINE 1(50%)@PQ-Si (M25) presents a viable carrier for the use case of C4C considering slow CO₂ desorption rates in a cement environment, where further investigation into this material is warranted.

Amine-grafted silicas

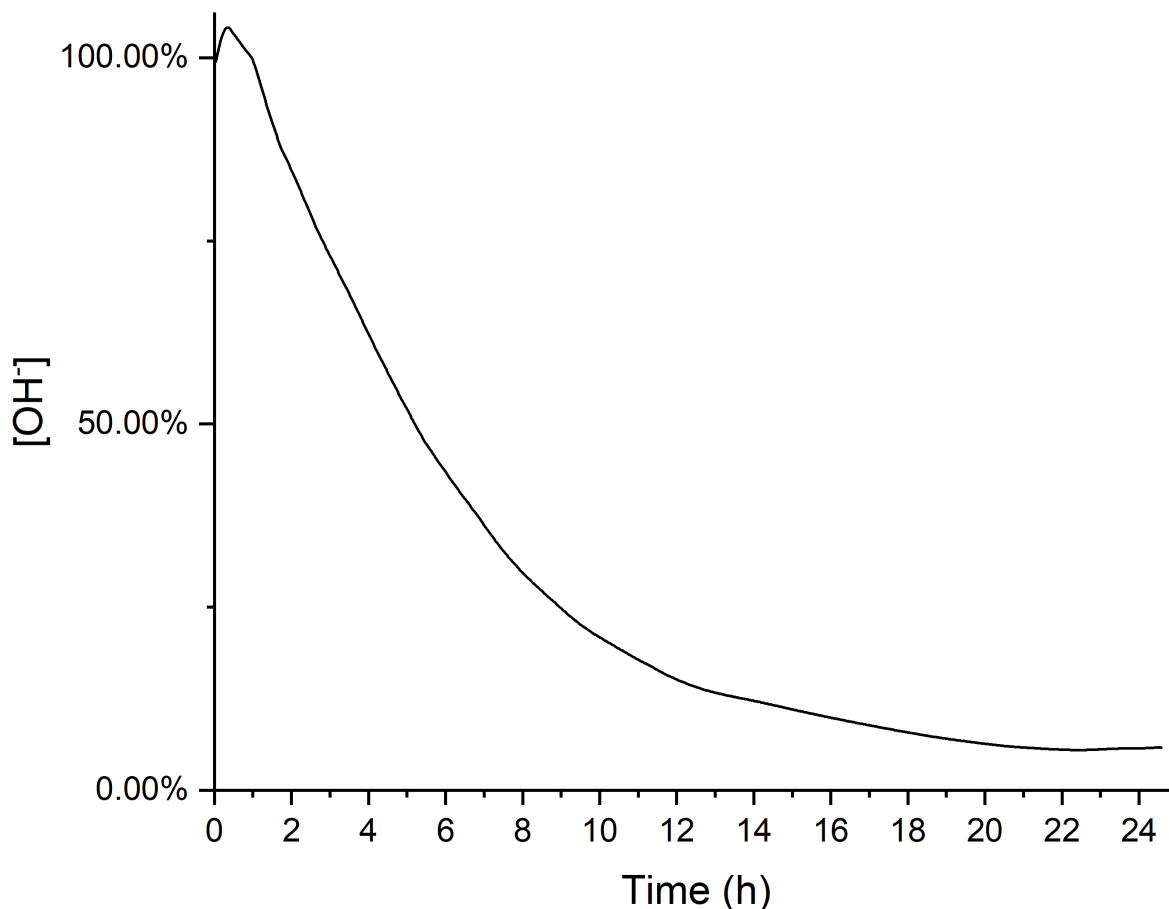
CO₂ loaded amine-grafted silica carriers were also examined for desorption in simulated cement solutions. AMINE 3.1@Si_0.30 showed the slow desorption kinetics under a nitrogen atmosphere (Table 3), and the [OH⁻] evolution of the simulated solution with the addition of this carrier loaded with CO₂ is shown in Figure 19.

Figure 16: [OH⁻] Consumption profile of a simulated cementitious solution prepared with the addition of CO₂ loaded AMINE 3.1@Si_{0.30}



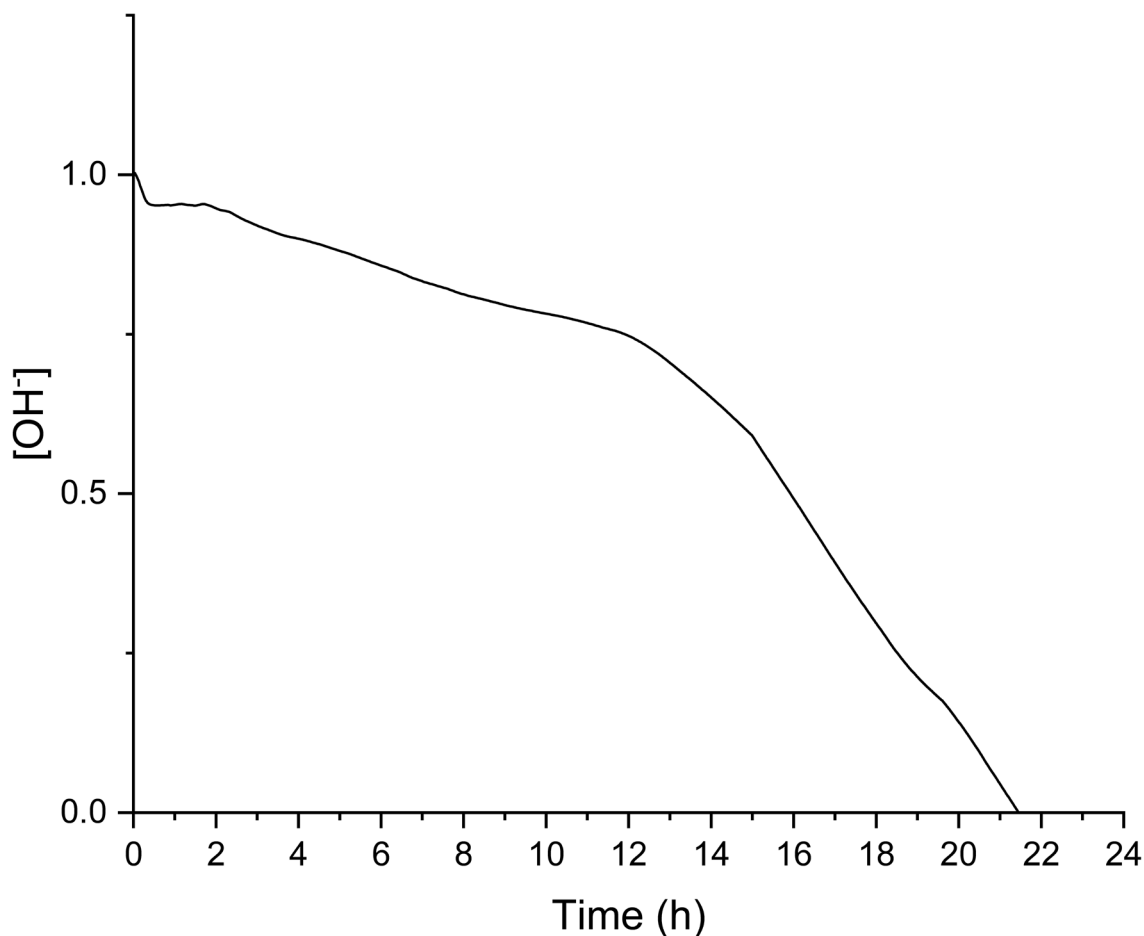
While showing slow CO₂ desorption under nitrogen, desorption from CO₂ loaded AMINE 3.1@Si_{0.30} in a Ca(OH)₂ simulated cementitious solution proceeds readily. [OH⁻] concentration is stable at a negligible quantity after 19 hours, which is likely to represent complete desorption of CO₂ from the carrier if temperature correction was taken into account here. The rapid desorption of CO₂ from AMINE 3.1@Si_{0.30} when considering the performance of AMINE 3.1@Si carriers was interesting, considering it was a high performing material of this class in terms of slow desorption under nitrogen, but was not necessarily an indication that all variants of this carrier would show rapid desorption. For example, [OH⁻] consumption (and CO₂ desorption) from loaded AMINE 3.1@Si_{0.30} was slower than observed with CO₂_AMINE 1(40%)@PQ-Si (M8) and CO₂_AMINE 2(50%)@PQ-Si, but the latter materials showed advantageous desorption rates under nitrogen. There is evidently a complex mechanism of CO₂ desorption in simulated cementitious solutions, depending on the class of carrier added. The [OH⁻] evolution profile of a simulated cement solution with the addition of AMINE 3.1@Si_{0.35}, a carrier which showed more facile CO₂ desorption under nitrogen than AMINE 3.1@Si_{0.30}, is shown in Figure 20.

Figure 17: [OH⁻] Consumption profile of a simulated cementitious solution prepared with the addition of CO2 loaded AMINE 3.1@Si_{0.35}



While AMINE 3.1@Si_{0.35} showed faster CO₂ desorption kinetics than AMINE 3.1@_0.30 under nitrogen (Table 3), in a simulated cementitious solution desorption was more labile. After a 24 hour period stirring in the simulated cementitious Ca(OH)₂ solution, ~6 % of previously adsorbed CO₂ was still present on AMINE 3.1@Si_{0.35}. The consumption of [OH⁻] in this mixture presented a similar, but less exaggerated profile to that observed in the mixture with AMINE 3.1@Si_{0.30}, where the initial rate of CO₂ desorption from the carrier is fast, but slows over time until a constant level of hydroxide is present towards the end of the experimental measurement. The results presented in Figures 19 and 20 indicate that the topologies AMINE 3.1@Si_{0.30} and AMINE 3.1@Si_{0.35} are similar, with the accessibility of adsorbed CO₂ to hydroxide being lower for the latter carrier. This may arise as a result of a greater proportion of grafted AMINE 3.1 being present within the pores of the silica, with bound CO₂ that is less accessible to hydroxide if significant blockage of the pores by surface-grafted AMINE 3.1 is taking place. An interplay between adsorption capacity of the carrier and hydroxide ion accessibility to the adsorbed CO₂ may be important in carrier performance in cement based off of these rationalisations. CO₂ loaded AMINE 3.1@Si_{0.45} was also examined for CO₂ release through measurement of [OH⁻] in a simulated cementitious solution, with the results highlighted in Figure 21.

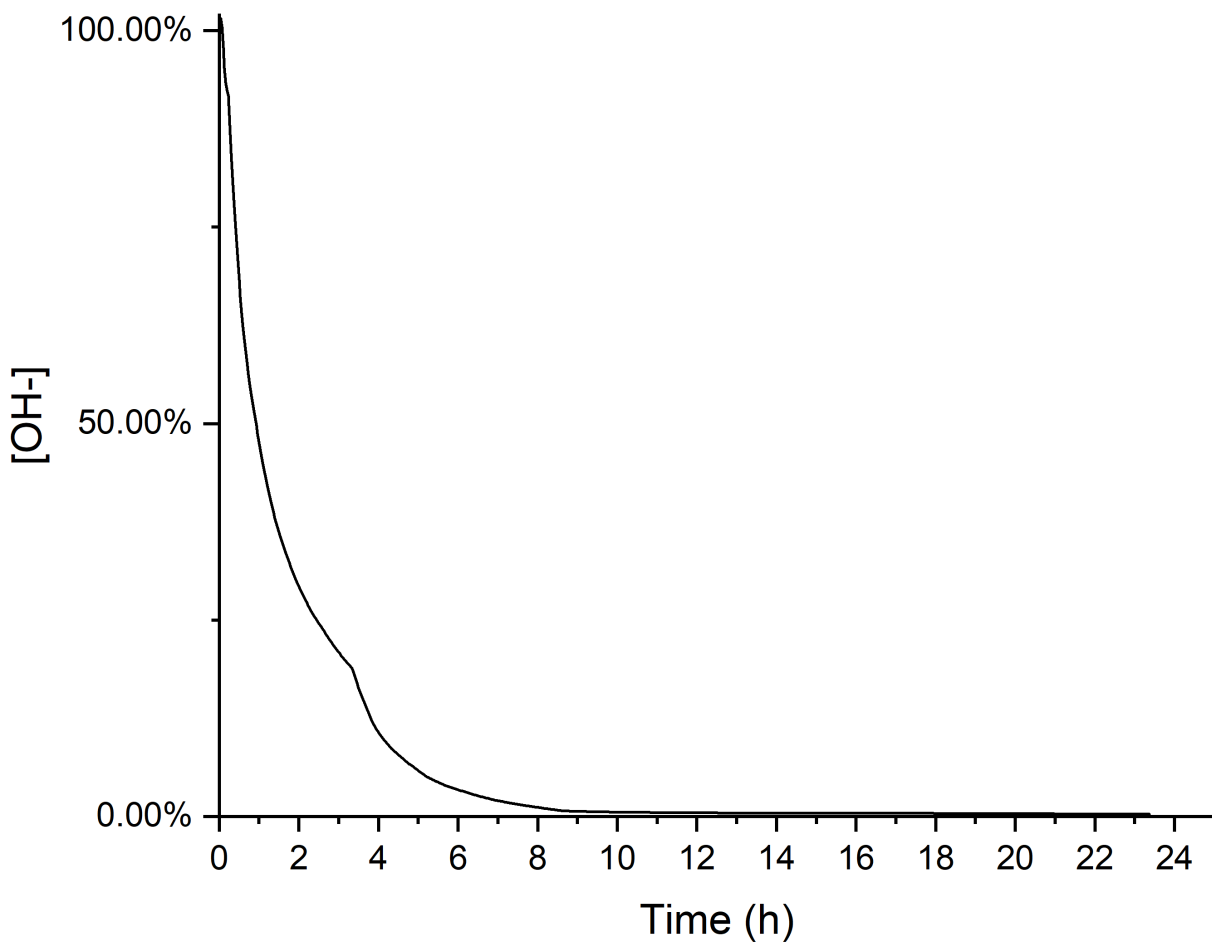
Figure 18: [OH⁻] Consumption profile of a simulated cementitious solution prepared with the addition of CO₂ loaded AMINE 3.1@Si_{0.45}.



Of the AMINE 3.1@Si analogues that were examined for CO₂ desorption in a simulated cementitious solution, AMINE 3.1@Si_{0.45} was the optimum carrier considering rate of CO₂ desorption. What was of interest from the [OH⁻] consumption curve presented in Figure 21 was the shape, where the profile of consumption was significantly different to those presented in Figures 19 and 20. Initial consumption of hydroxide was slow, indicating that over short durations in basic conditions, the CO₂ that was previously loaded to AMINE 3.1@Si_{0.45} was largely retained. After an induction period of 12 hours, rate of CO₂ release from the carrier increased significantly, where a constant concentration was measured after 20.5 hours. CO₂ desorption from AMINE 3.1@Si_{0.30} and AMINE 3.1@Si_{0.35} in the simulated cementitious solution was initially very fast, then slowed over time (according to the [OH⁻] consumption curves presented in Figure 19 and Figure 20 respectively), while Figure 21 presents significantly different CO₂ desorption kinetics from AMINE 3.1@Si_{0.45} in the same environment. The nature of grafted CO₂ loaded AMINE 3.1 on AMINE 3.1@Si_{0.45} is evidently different to the same functional groups present on AMINE 3.1@Si_{0.30} and AMINE 3.1@Si_{0.35}, resulting in significant difference in CO₂ desorption mechanism. The majority of chemisorbed CO₂ present on AMINE 3.1@Si_{0.45} may be present as AMINE 3.1 that is grafted within the pores of the mesoporous silica support, and if an extremely large amount of pore blockage is preventing the access of hydroxide to within the pores the support, then cleaving of surface grafted AMINE 3.1 would have to take place before the desorption of CO₂

within the pores could proceed. This forms a rational explanation of the presence of an induction period of slow $[\text{OH}^-]$ consumption in the simulated cementitious solution containing CO2 loaded AMINE 3.1@Si_0.45, before rapid CO2 desorption from the carrier takes place. This further gives highlights that the nature of AMINE 3.1 grafting topology is incredibly important when considering desorption kinetics in cement conditions, and how fast CO2 desorption under nitrogen (Table 3) does not necessarily correlate to carriers that lose CO2 the fastest in a simulated cement environment. Amine 3.5@Si, an amine-grafted carrier with the slow CO2 desorption rates observed under a nitrogen atmosphere (Table 3), was also examined for CO2 desorption in a simulated cementitious environment, with the $[\text{OH}^-]$ consumption of this solution shown in Figure 22.

Figure 19: $[\text{OH}^-]$ Consumption profile of a simulated cementitious solution prepared with the addition of CO2 loaded Amine 3.5@Si



Of all the amine-grafted carriers examined in 3.2.2.2 for CO2 desorption in a cementitious simulated $\text{Ca}(\text{OH})_2$ environment, Amine 3.5@Si exhibited the fastest desorption time. Complete consumption of hydroxide in the solution with CO2 loaded Amine 3.5@Si had taken place after 12 hours. This even further highlights that the topology of grafted material on silica is of paramount importance when considering CO2 desorption rates in cementitious environments, as from the results in Table 3 alone, Amine 3.5@Si would be considered to be the carrier the second slowest CO2 desorption kinetics (under N_2). However, from the simulated cementitious experiments conducted in 3.2.2.2, we know that in conditions more aligned to the final use case of a carrier by C4C, that it actually the worst performing carrier

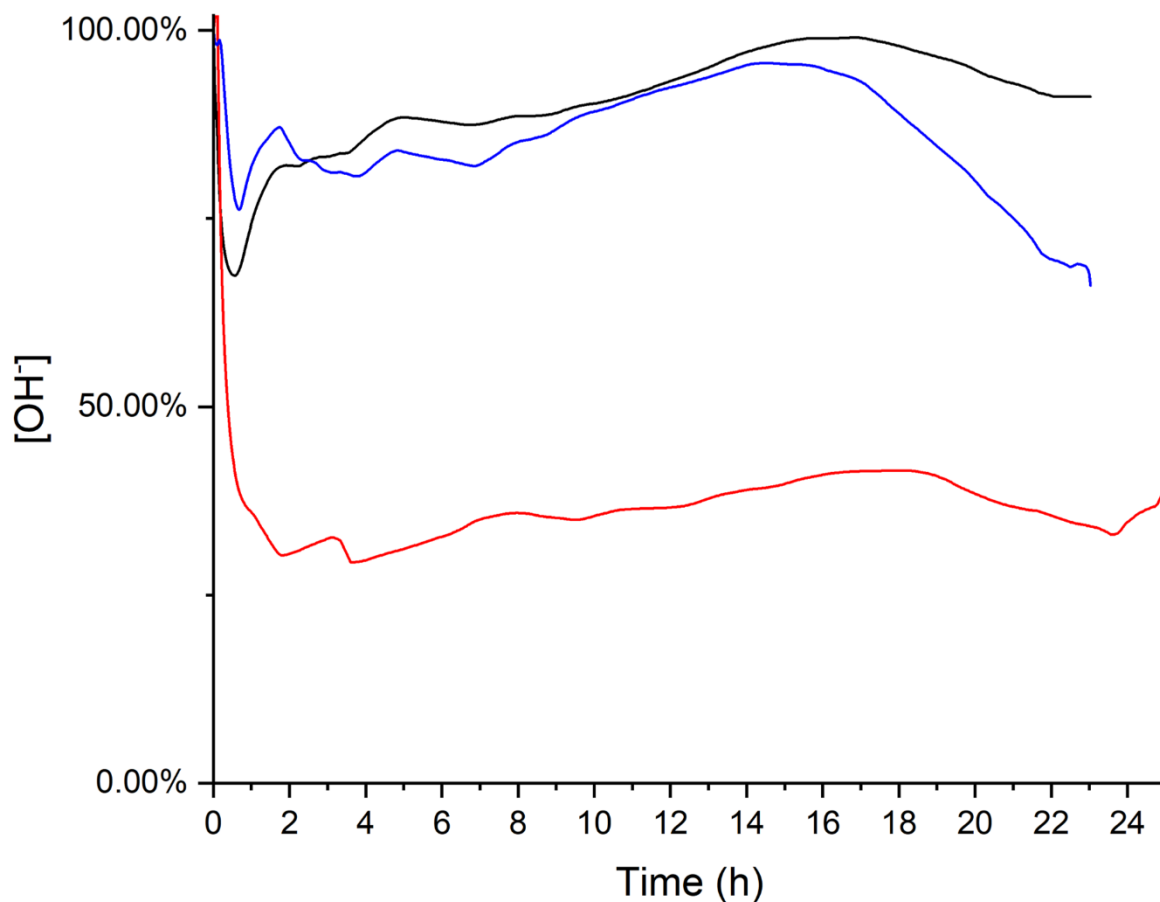
regarding CO₂ desorption speed. Further investigation into carrier topology would give better understanding as to the nature of CO₂ desorption in cement conditions from the amine-grafted silica class of carrier, where Amine 3.5@Si would be predicted to show a uniform distribution of grafted Amine 3.5, where hydroxide would be readily be available to diffuse into the pores of the silica support.

The results presented in 3.2.2.2 on the addition of CO₂ loaded amine-grafted silicas to simulated cement solutions give an interesting insight into how previously evaluated carrier desorption performance under nitrogen does not translate to how desorption from the same carriers proceed under basic cementitious conditions. Further investigation into carrier topology would further support the hypotheses outlined here.

Amine-impregnated Polymer 1-AMINE 3 carriers

Identical to the simulated cementitious solution experiments conducted in 3.2.2.1 and 3.2.2.2 with amine impregnated and amine-grafted carriers respectively, Ca(OH)₂ solutions with CO₂ loaded amine-impregnated Polymer 1-AMINE 3 carriers were analysed for hydroxide consumption, to determine CO₂ release rates from these carrier materials. [OH⁻] consumption curves for different simulated cementitious solutions loaded with POLYMER 1 AMINE 3Amine 3.4, POLYMER 1 AMINE 3-AMINE 1 and POLYMER 1 AMINE 3-AMINE 3 are shown in Figure 23.

Figure 20: [OH⁻] Consumption profiles of simulated cementitious solutions prepared with the addition of CO₂ loaded POLYMER 1 AMINE 3Amine 3.4 (black), POLYMER 1 AMINE 3-AMINE 1 (red) POLYMER 1 AMINE 3-AMINE 3 (blue).



Unlike with amine-impregnated and amine grafted silicas, the simulated cementitious solution study conducted here for CO₂ loaded amine-impregnated Polymer 1-AMINE 3 carriers was not a feasible way to evaluate CO₂ release from the carriers by monitoring [OH⁻] consumption. The [OH⁻] consumption of POLYMER 1 AMINE 3-AMINE 1 appears to indicate an initial rapid release of CO₂ to the system, followed by a minor fluctuation of hydroxide concentration in the system around the same level as observed after the initial rapid loss after 1.5 hours (Figure 23). However, when the consumption of hydroxide in the simulated cementitious solutions with CO₂ loaded POLYMER 1 AMINE 3Amine 3.4 and POLYMER 1 AMINE 3-AMINE 3 are considered, it is apparent that this experiment cannot be used to rationalise CO₂ release from the amine-impregnated Polymer 1-AMINE 3 carrier class. These [OH⁻] evolution curves are sporadic, with frequent decreases and increases in [OH⁻], in a closed system where the generation of [OH⁻] from previously consumed material is not possible. The POLYMER 1 AMINE 3-Amine class of carrier can break down under the simulated cementitious solution environment, releasing AMINE 3 into the system. As AMINE 3 is a strongly basic material, its release into the simulated cementitious solution will increase pH, hence using solution pH as a tool to calculate [OH⁻] in the system is fundamentally flawed. As a result, the [OH⁻] calculated from pH monitoring in the experiments described in the curves shown in Figure 23 to calculate CO₂ release from these carriers are not representative of the actual concentration of hydroxide

in the system, hence this method cannot be used to evaluate CO₂ release rates from amine-impregnated Polymer 1-AMINE 3 carriers.

Conclusions and targeted optimisations based on results

A detailed screen of a wide range of potential CO₂ carriers identified for use by C4C has been undertaken in WP-3.1, highlighting interesting results on CO₂ desorption performance in a cement simulated solution environment.

From previous study in Work Packages 1 and 2, three classes of carrier showed the highest potential to fit the use cases of C4C, those being high CO₂ capacities and slow CO₂ desorption rates. Amine-impregnated silicas, amine grafted silicas and amine-impregnated Polymer 1-AMINE 3 carriers have all been shown to exhibit CO₂ adsorption capacities above the threshold to be considered by C4C, while all showing slow CO₂ desorption rates under nitrogen. What was still unknown was whether these slow desorption rates that had previously been evaluated would translate to similar results in an environment more representative of that of cement, i.e. basic. Through stirring CO₂ loaded carrier materials in Ca(OH)₂ solutions of concentration designed to mimic that of 7-day old cement, CO₂ desorption rates from various carrier materials could be rationalised through constantly monitoring pH variation, calculating the concentration of hydroxide ions in the solution, and equating this to the amount of CO₂ that had desorbed from the carrier at any given time.

In prior studies, amine-impregnated silicas were shown to be high capacity carrier materials with slow CO₂ desorption regardless of the nature of the impregnated amine. CO₂ Loaded mesoporous silicas impregnated with AMINE 2, AMINE 1 (M8) and AMINE 1 (M25) all demonstrated rapid desorption under a nitrogen atmosphere, however, study in WP-3.1 showed that slow desorption under nitrogen did not necessarily translate to slow CO₂ desorption in a simulated cement environment. The size of the impregnated amine has been shown to play a vital role in how this class of carrier performs in a simulated cementitious solution with regards to slow CO₂ desorption kinetics. Simulated Ca(OH)₂ solutions with silicas impregnated with small CO₂ loaded polyamines (AMINE 2 and M8 AMINE 1) showed rapid decrease in hydroxide concentration, which was indicative of the rapid release of CO₂ from the respective carrier materials. While CO₂ loaded silica impregnated with the larger, M25 derivative of AMINE 1 showed advantageous CO₂ desorption kinetics to those impregnated with the smaller amines, with desorption becoming more rapid as the quantity of impregnated material increased. It is evident that hydroxide diffusion into the pores of the mesoporous silica, to access adsorbed CO₂ to react to form carbonate, is a key determining factor in the rate of CO₂ desorption from amine-impregnated silicas in a simulated cementitious solution environment. With less sterically bulky carbonated amine (AMINE 2 and Mw-800 AMINE 1) impregnated in the mesoporous silica, hydroxide is evidently more accessible to react with adsorbed CO₂, leading to the rapid decrease in simulated solution hydroxide concentration observed in Figures 14 and 15. Slower CO₂ desorption rates from the carbonated AMINE 1@PQ-Si (Mw-25,000) analogues are readily explained by the increased steric bulk of the

impregnated materials limiting the diffusion of hydroxide through the pores of the mesoporous silica support, slowing the formation of calcium carbonate in the system. The slower desorption of CO₂ from AMINE 1(50%)@PQ-Si (M25, Figure 17) compared to AMINE 1(40%)@PQ-Si (M25, Figure 16) further justifies this rationalisation, as the analogue with a higher loading of impregnated AMINE 1 showed the slowest desorption kinetics. Of the materials examined here, AMINE 1(50%)@PQ-Si showed the optimum CO₂ desorption kinetics in simulated cementitious solution testing, hence further study will be conducted on this material.

From prior study, amine-grafted silicas also presented a class of carrier with high adsorption capacities with slow desorption rates, where carrier properties could be readily tuned by changing the quantity of water in the synthesis of the material. AMINE 3.1@Si carriers with different desorption characteristics under nitrogen (Table 3) were studied in WP-3.1 to evaluate desorption rates under simulated cementitious solution conditions. Interestingly, this study showed that slow desorption rates of this class of carrier under nitrogen did not necessarily translate to slow CO₂ desorption in a basic simulated cementitious solution. For example, of the three AMINE 3.1@Si analogues studied in this trial, AMINE 3.1@Si_{0.30} showed the slow rates of CO₂ desorption under nitrogen (Table 3), but when the [OH⁻] consumption curves in Figures 19, 20 and 21 are considered, this carrier showed the fastest CO₂ desorption under simulated cementitious solution conditions. Again, Amine 3.5@Si showed slow desorption kinetics under nitrogen (Table 3), but in a basic simulated cementitious solution, [OH⁻] consumption was facile (Figure 22). Interesting differences in the profiles of hydroxide consumption in the simulated solutions with CO₂ loaded AMINE 3.1@Si carriers were also observed, where AMINE 3.1@Si_{0.45} showed a significant induction period before rapid consumption of hydroxide took place (Figure 21), while solutions with CO₂ loaded AMINE 3.1@0.30 (Figure 19) and AMINE 3.1@0.35 (Figure 20) both showed an initial rapid consumption of hydroxide on addition of the carrier. These results highlight that the topology of grafted amine to silica carriers is of vital importance when considering CO₂ desorption from these materials in a basic cementitious environment, an observation that could not be made from prior studies in WP1 and WP2 on CO₂ desorption from these materials under nitrogen. Rationalisations into potential different surface grafting topologies on these materials have been elaborated on in 3.2.2.2, to explain the differences in CO₂ desorption of the amine-grafted silica carriers in simulated solutions that were observed. As all amine-grafted silica carriers examined here showed near complete desorption of CO₂ in simulated cementitious solutions, they are not a viable class of carrier moving forward by C4C for use in cement.

While the simulated cementitious solution experiments conducted in WP-3.1 were viable methods of evaluating the desorption of CO₂ from amine-impregnated and amine-grafted silica carriers, amine-impregnated Polymer 1-AMINE 3 carriers could not be analysed for CO₂ desorption in a simulated solution via the same methodology. Hydroxide consumption profiles for POLYMER 1 AMINE 3Amine 3.4, POLYMER 1 AMINE 3-AMINE 1 and POLYMER 1 AMINE 3-AMINE 3 (Figure 23) showed significant variations (both increases and decreases) in hydroxide consumption. As the polymer support breaks down under basic conditions to form AMINE 3, a highly basic material, the solution pH increases, hence using this value to calculate solution hydroxide concentration and from that, CO₂ desorption from the suspended carrier become unfeasible. Further investigation on method development to rationalise the nature of

CO2 desorption from amine-impregnated Polymer 1-AMINE 3 class of carrier in basic simulated solutions is required before any judgement on potential performance of these carriers in cement can be made.

Carrier optimisations based on results

POLYMER 1 AMINE 3-AMINE 1, POLYMER 1 AMINE 3-AMINE 3, and POLYMER 1 AMINE 3Amine 3.4 were evaluated as a family of carriers utilising a combination the ligand and base AMINE 3 in conjunction with another amine utilising their combined benefits. A precursor of Polymer 1 was utilised as the carrier based. These carriers showed some promise initially, however the uncertainty with regards to release rate as well as potential behaviour in concrete render them unsuitable due to higher level of risk associated with them. Their performance is unreliable, making them ineffective for practical use. Additionally, large-scale production is complex due to potentially rare materials, intricate manufacturing, or specialised equipment. Finally, their Polymer 1 composition raises environmental concerns, as they could become a source of microplastic pollution upon disposal or demolition. This has to be studied in far more details which are out with the scope of this project.

As several amine impregnated silica class carriers exhibited optimal CO2 desorption profiles (in excess of 48 hours, the focus was then on optimising and developing the amine-grafted carrier class. Given how the results detailed in section 4.4 of this report highlight the dependence on OH- diffusion and incorporation into the pores of the solid supports, and given how sensitive the CO2 release appears to be on the nature of the amine speciation, a clear route to optimisation as a result of work performed in this work package was to modulate the solid support to effect **reduced access of OH- to the CO2 bound species on the amine grafted carriers**. A key way to achieve this is the use of a less Lewis acidic (n.b. Lewis acidity pertains to a materials donating or accepting ability, rather than the concepts of acidity/basicity discussed earlier) substrate. Silica is particularly Lewis acidic, to by reducing this effect the affinity for electron donor species (such as OH-) can be greatly reduced by utilising an alternative substrate with a lower Lewis acidity, such as alumina (P1).

Literature review

When considering alternative support materials for the covalent grafting of amines, towards CO2 capture devices for use by C4C, P1 is an ideal option.

Considering availability, alumina is also a viable option for the basis of a amine-grafted carrier for production on a large scale, as aluminium is the third most abundant element in the earth's crust.

P1 can come in many forms, but through reviewing literature, alumina nanoparticles were identified as a viable support material for amine grafting towards CO2 capture devices for the specific use case of C4C (addition to concrete).

Alumina has also been shown in previous literature studies to act as a feasible support for the grafting of amine 3.4, in the formation of analogous materials to silica supported amines that have previously been studied for CO₂ adsorption by C4C. Jin et al. for example demonstrated the successful covalent grafting of amine 3.1, as well as diamino and triamino derivatives to mesoporous alumina.¹ Immobilisation of silyl amines on mesoporous alumina has also been investigated by Grossman et al., where interestingly, they studied the use of this class of material for the direct air capture of CO₂. The group studied the grafting Amine 3.1 to two classes of alumina support (industrial alumina pellets and monolithich alumina), and demonstrated the efficacy of these materials in CO₂ capture.² The use of amine-grafted alumina materials for the adsorption of CO₂ was also studied by Potter et al. who demonstrated that both ordered and disordered alumina could be used as supports for Amine 3.2 with high loadings, and that these materials were effective devices for the adsorption of CO₂.³

As P1 nanoparticles have been shown to be beneficial additives to cement to improve compressive strength, and because alumina has been shown to be a viable support for the grafting of alkoxysilyl-amines for CO₂ capture devices, amine-grafted P1 nanoparticles were identified as a optimisation candidate for the amine-grafted carrier class for C4Cs use case.

AMINE 3.1@P1

As 3-aminopropyl trimethoxy silane (AMINE 3.1) had been well studied for grafting onto silica by C4C, initial preparations of AMINE 3.1@P1 were tested using this grafting agent. These carrier materials would be analysed by thermal decomposition TGA to determine the surface loadings of covalently bound amine to the alumina nanoparticles, and by high pressure CO₂ adsorption to determine CO₂ adsorption capacity. The best performing carriers for high pressure CO₂ adsorption would be examined by TGA CO₂ sorption, to determine CO₂ desorption kinetics under a nitrogen atmosphere.

Synthesis

Three different analogues of AMINE 3.1@P1 was prepared according to different literature procedures, to optimise the performance of this class of carrier for CO₂ adsorption capacity. For clarity, these materials have been labelled AMINE 3.1@P1-1, AMINE 3.1@P1-2 and AMINE 3.1@P1-3.

Synthesis of AMINE 3.1@P1-1

P1 Powder(1.00g) was dispersed in toluene (100 mL) for ~30 minutes, after which AMINE 3.1 (3.6 mL) and AMINE 3 (6 mL) were added. The reaction mixture was stirred at 70 °C for ~18 hours. On cooling, approximately 1/2 of the reaction supernatant solution was removed via syringe, and the solid product was isolated via centrifugation (15 min, 4500 rpm). The product

¹ X. Jin, W. Cai and Z. Cai, RSC Adv, 2017, 7, 53076–53086

² Q. Grossmann, V. Stampi-Bombelli, A. Yakimov, S. Docherty, C. Copéret and M. Mazzotti, Ind Eng Chem Res, 2023, 62, 13594–13611

³ M. Potter, K.M Cho, J.J Lee, C.W Jones, ChemSusChem, 2017, 10, 2192-2201

was washed 3 times via a cycle of sonication (15 min) in toluene (~20 mL) followed by centrifugation (15 min, 4500 rpm).

Synthesis of AMINE 3.1@P1-2

P1 Powder(1.00 g) was added to a mixture of toluene (100 mL), H₂O (0.25 mL) and AMINE 3.1 (3.6 mL), and the reaction mixture was stirred for ~25 minutes at room temperature. The temperature was raised to 70 °C and the reaction was stirred for ~18 hours. On cooling, approximately 2/3 of the reaction supernatant solution was removed via syringe, and the solid product was isolated via centrifugation (15 min, 4500 rpm). The product was washed 3 times via a cycle of sonication (15 min) in toluene (~20 mL) followed by centrifugation (15 min, 4500 rpm).

Synthesis of AMINE 3.1@P1-3

Three centrifuge tubes were each charged with toluene (~33.3 mL), P1 powder(1.00 g split approximately across the three tubes) and AMINE 3.1 (1.2 mL). The tubes were sonicated for 30 minutes, and the contents were added to a flask that was stirred at 70 °C for ~18 hours. On cooling, approximately 2/3 of the reaction supernatant solution was removed via syringe, and the solid product was isolated via centrifugation (15 min, 4500 rpm). The product was washed 3 times via a cycle of sonication (15 min) in toluene (~20 mL) followed by centrifugation (15 min, 4500 rpm).

Figure 24: Synthesis of AMINE 3.1@P1 analogues



Figure 21: AMINE 3.1@P1 synthesis during- (left) and post-reaction (right)

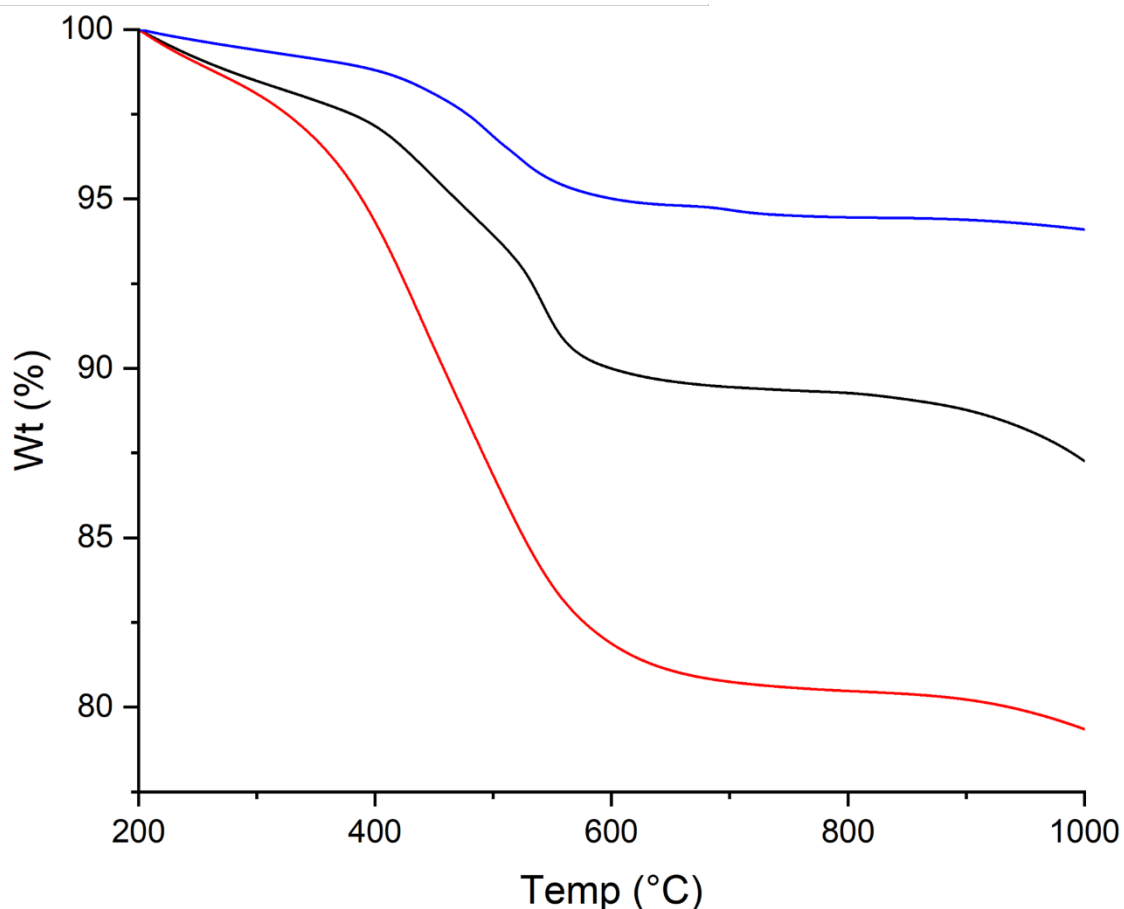
Characterisation – Thermal decomposition

The three AMINE 3.1@P1 analogues prepared according to 4.3.2.1 were analysed by TGA for thermal decomposition, where the loss in sample mass between the temperature region of 200-800 °C was used to calculate the quantity of AMINE 3.1 that was covalently grafted to the surface of the P1 nanoparticles (Table 4).

Table 4: Amine loadings of AMINE 3.1@P1 carriers prepared according to 4.5.2.1

Sample	Amine loading / wt%	Amine loading/ mMol g ⁻¹
AMINE 3.1@P1-1	10.73	1.88
AMINE 3.1@P1-2	19.53	3.43
AMINE 3.1@P1-3	5.55	0.97

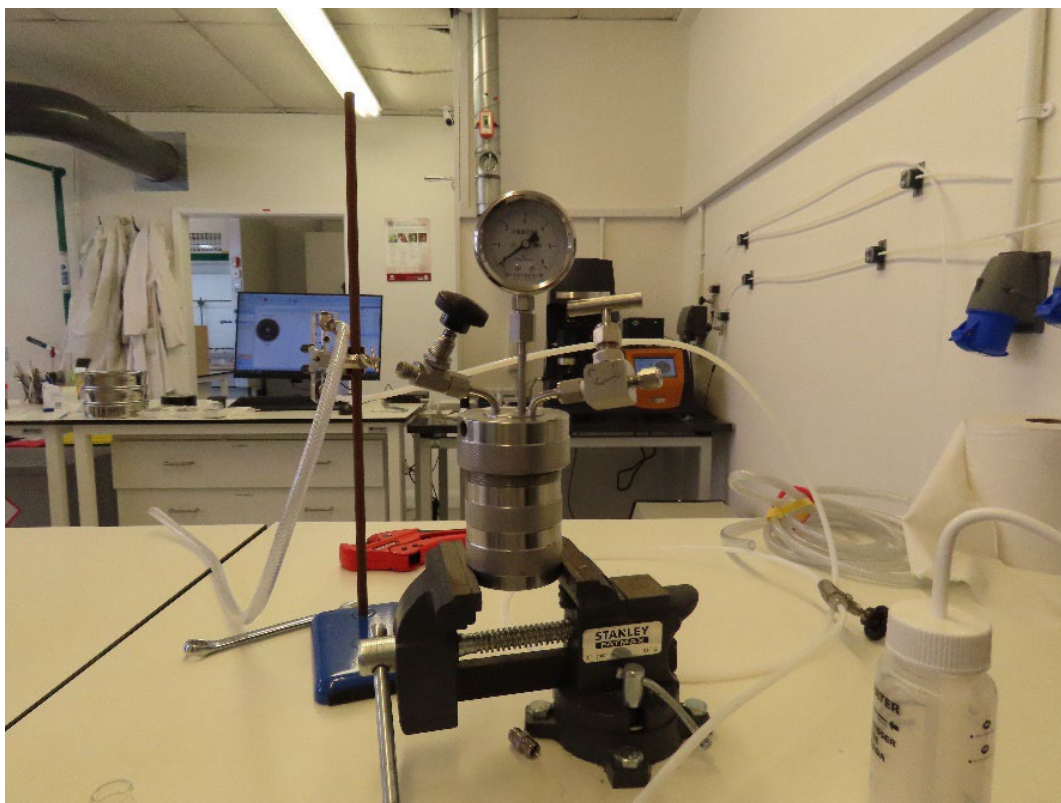
Figure 22: Thermal decomposition traces of AMINE 3.1@P1-1 (black), AMINE 3.1@P1-2 (red), AMINE 3.1@P1-3 (blue)



All three AMINE 3.1@P1 syntheses were conducted using toluene as a reaction solvent, at a temperature of 70 °C, but AMINE 3.1@P1-2 demonstrated a significantly higher surface loading of AMINE 3.1 than AMINE 3.1@P1-1 and AMINE 3.1@P1-3. The preparation of AMINE 3.1@P1-2 was the only one that utilised a small loading of H₂O, which, in the preparation of amine-grafted silicas, is known to improve surface loadings through hydrolysis of the methoxy silane groups of AMINE 3.1 to generate reactive silanol groups that can readily react with the silica surface. AMTPS@P1-3 showed the lowest AMINE 3.1 surface loading of the three derivatives that were prepared, while the analogue prepared with the addition of triethylamine (AMINE 3.1@P1-1) possessed a higher surface loading than the derivative prepared with no additive (AMINE 3.1@P1-3), but a lower loading than that prepared with the addition of water (AMINE 3.1@P1-2).

Characterisation – High pressure CO₂ adsorption

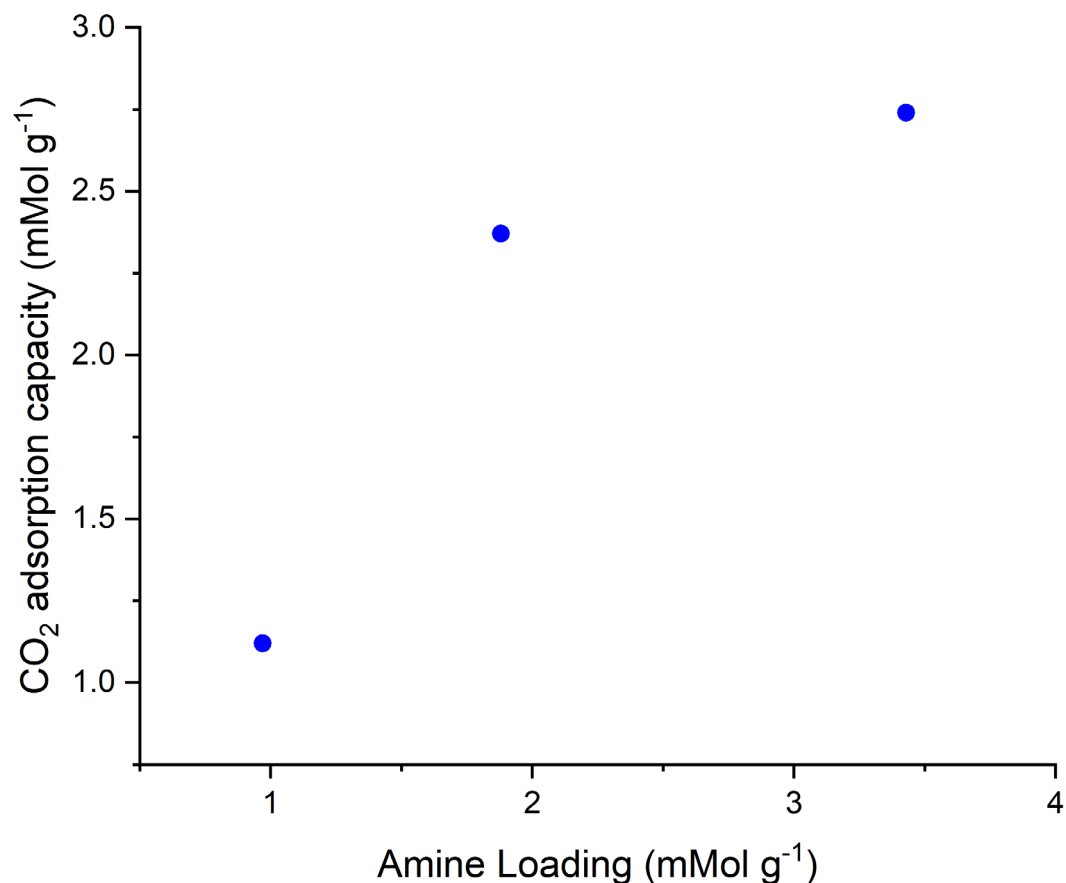
The three AMINE 3.1@P1 derivatives prepared according to 4.3.2.1 were analysed for CO₂ adsorption capacities through high pressure exposure. The AMINE 3.1@P1 analogues were added to an autoclave, which was pressurised with 10 bar CO₂. The pressurised autoclave was heated at 70 °C overnight, where on cooling to room temperature and release of the CO₂ pressure, the difference in mass between the carrier before and after CO₂ loading was used to calculate adsorption capacity. The CO₂ adsorption capacities of AMINE 3.1@P1-1, AMINE 3.1@P1-2 and AMINE 3.1@P1-3 are reported in Table 5.

Figure 23: Autoclave used for high pressure carrier CO2 loading**Table 5: CO2 Adsorption capacities of AMINE 3.1@P1 carriers prepared according to 4.5.2.1 (10 bar CO2, 70 °C, overnight).**

Sample	CO2 capacity (mMol g ⁻¹ / wt %)
AMINE 3.1@P1-1	(2.37 / 10.42)
AMINE 3.1@P1-2	(2.74 / 12.08)
AMINE 3.1@P1-3	(1.12 / 4.93)

The adsorption capacities of the AMINE 3.1@P1 analogues correlate with the surface loadings of AMINE 3.1 that are present on these materials, where AMINE 3.1@P1-2 (highest amine loading) demonstrates the highest CO2 adsorption capacity, and AMINE 3.1@P1-3 (lowest amine loading) displays the lowest CO2 adsorption capacity. However, the trend isn't linear, as shown by the graph in Figure 28.

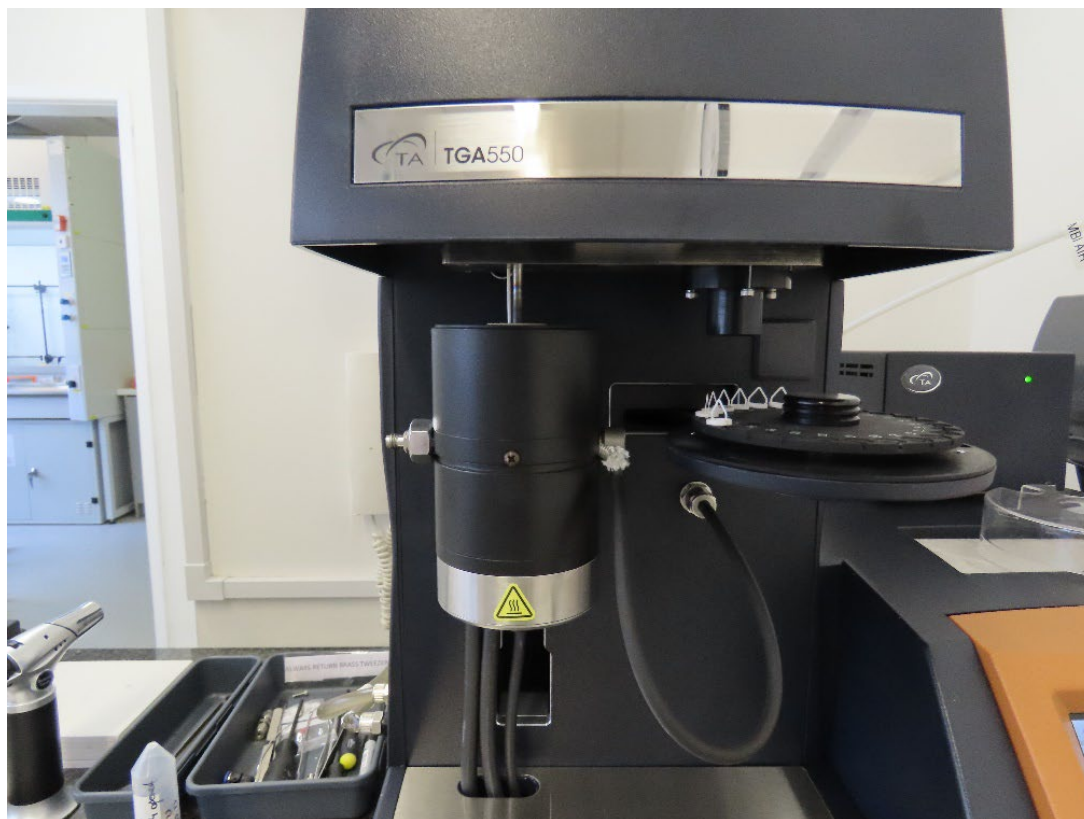
Figure 24: Comparing grafted amine loadings and CO₂ adsorption capacities of different AMINE 3.1@P1 carrier materials



As the amine loading on AMINE 3.1@P1 increases, CO₂ adsorption capacity also increases, but the rate of increase in capacity is decreasing as the amine loading increases. This gives an indication that a threshold CO₂ adsorption capacity for AMINE 3.1@P1 materials exists, where after a certain AMINE 3.1 loading is reached, further increases in CO₂ adsorption capacities will not be observed. Nanoparticle agglomeration with increased AMINE 3.1 loading may create a structure where access to grafted amines to CO₂ is not possible, giving a carrier with a maximum defined adsorption capacity that is governed by exposed grafted AMINE 3.1 on the surface of the carrier.

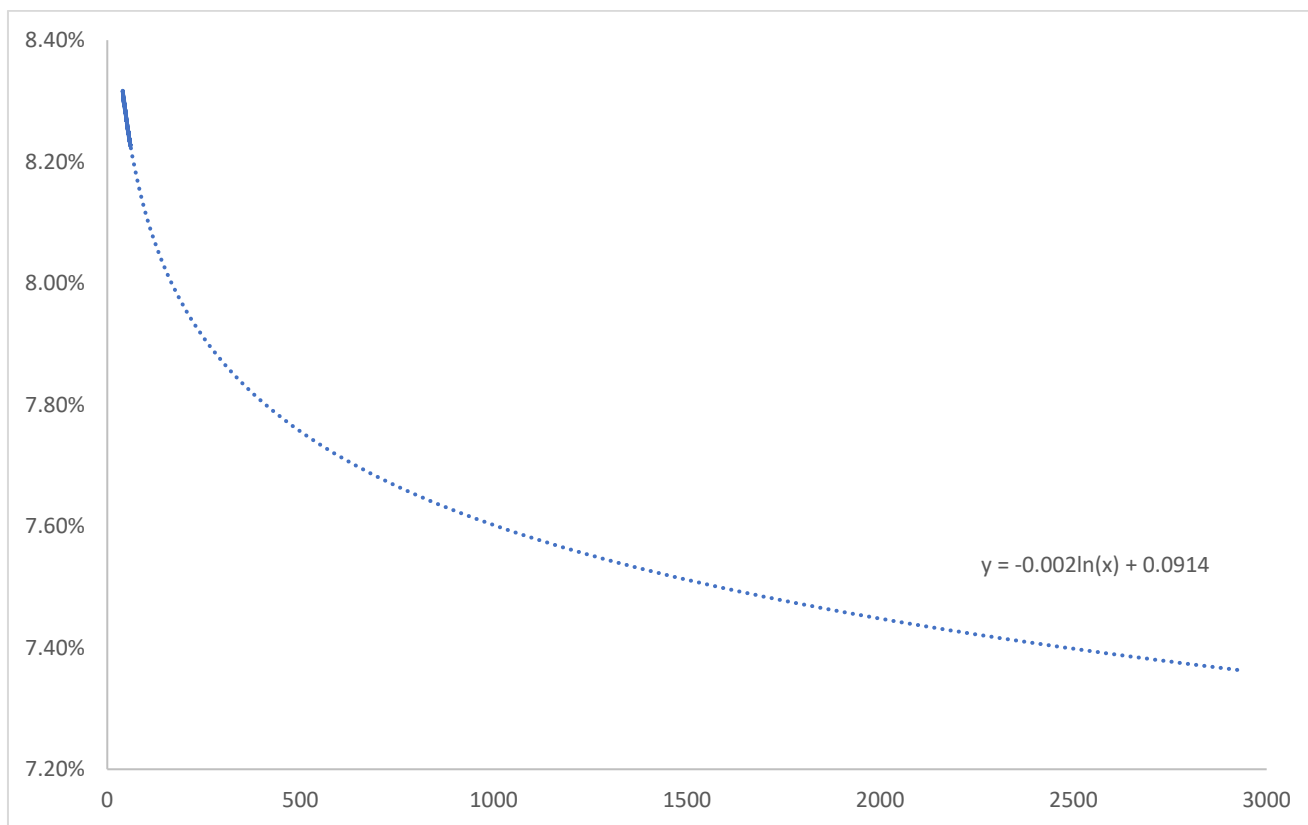
Characterisation – TGA CO₂ sorption

As the carrier with the highest CO₂ adsorption capacity determined by high pressure CO₂ adsorption, CO₂ sorption TGA was conducted on AMINE 3.1@P1-2. This was conducted according to the optimised CO₂ sorption TGA methodology developed in work package 2 (page 14). Adsorption capacities of AMINE 3.1@P1-2 via different modes are reported in Table 6.

Figure 25: TGA used for CO2 sorption analysis of carrier materials**Table 6: CO2 adsorption capacity (75 °C, 1 hour) of AMINE 3.1@P1-2 measured during TGA**

Sample	CO2 capacity / mMol g ⁻¹ (chemisorb)	CO2 capacity / wt% (chemisorb%)	Amine efficiency / %
AMINE 3.1@P1-2	2.07 (1.81)	9.10 (7.96)	52.8

From examining CO2 adsorption at both 75 °C and 25 °C, the majority of CO2 adsorption by AMINE 3.1@P1-2 could be determined to be via strong chemisorption, where 87.5% of the total adsorbed CO2 was adsorbed at 75 °C (this adsorption can be attributed to chemisorption). Desorption of CO2 from AMINE 3.1@P1-2 was also monitored, where an extrapolated desorption profile of CO2 from AMINE 3.1@P1-2 is shown in Figure 30.

Figure 26: Extrapolated desorption profile of CO2 from AMINE 3.1@P1 under N2 at 25 °C

As previously reported in Work Package 2 (page 18), where extrapolated desorption profiles of CO₂ from carrier materials were used to model adsorbed CO₂ quantities after 48 and 480 hours, the same procedure was used to model long-term CO₂ desorption from AMINE 3.1@P1-2. AMINE 3.1@P1-2 retains 76.4 % of previously adsorbed CO₂ after 48 hours, and 71.8 % of previously adsorbed CO₂ after 480 hours. The projected CO₂ retention of AMINE 3.1@P1-2 after 480 hours is higher than any AMINE 3.1@SiO₂ analogue that were reported in Work Package 2, and highlights the potential of AMINE 3.1@P1 to be an effective high capacity, slow CO₂ release carrier for use by C4C in cement.

Characterisation – Simulated solution CO₂ desorption

While AMINE 3.1@P1-2 was shown to exhibit labile CO₂ desorption kinetics under a nitrogen atmosphere, previous studies reported in Work Package 3 had shown that this would not necessarily translate to slow CO₂ release in a basic aqueous environment. It was of interest to investigate the rate of CO₂ desorption in simulated cementitious conditions from the alumina supported carriers prepared according to the procedures reported in 4.5.2.1, to rationalise whether the use of an alternative support material to silica for amine-grafted carriers would result in advantageous CO₂ desorption characteristics. The AMINE 3.1@P1 analogues prepared according to 4.5.2.1 were examined for CO₂ desorption in optimised simulated cementitious solution conditions, where solution hydroxide concentration could directly be equated to the rate of CO₂ release from the carrier (Figures 31, 32 and 34).

Figure 27: [OH⁻] Consumption profile of a simulated cementitious solution prepared with the addition of CO2 loaded AMINE 3.1@P1-1

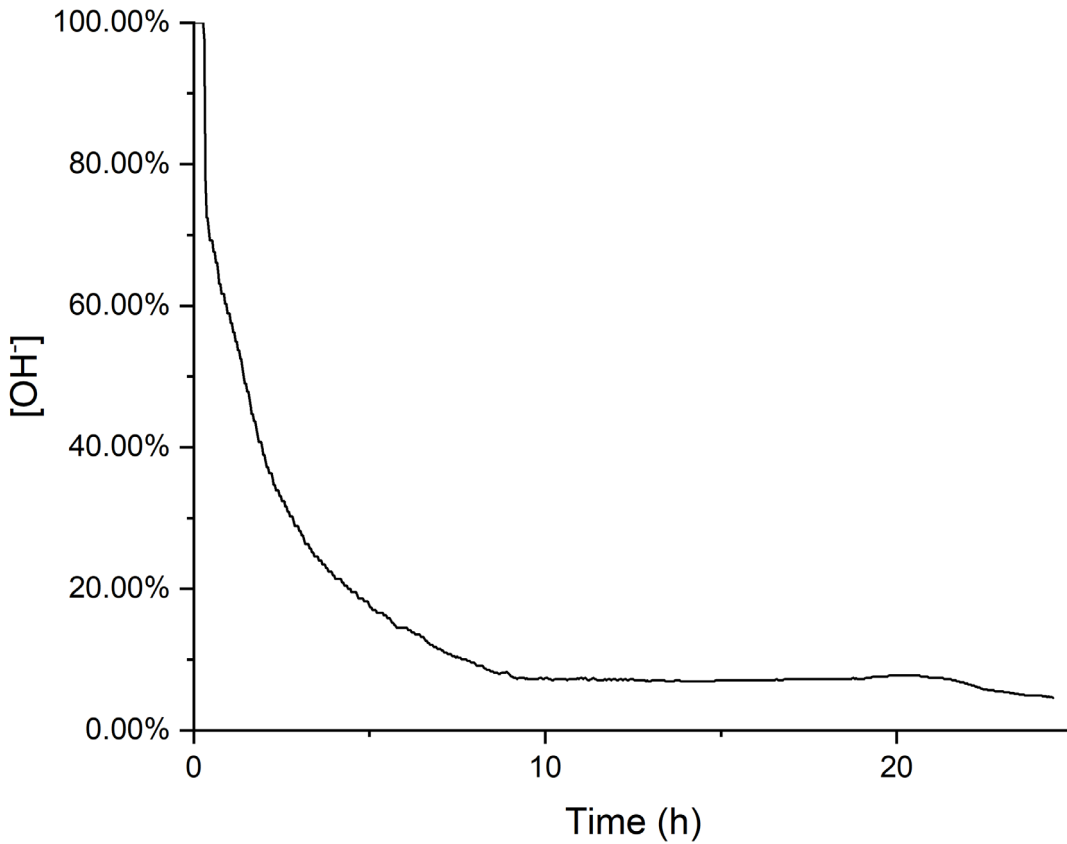


Figure 28: [OH⁻] Consumption profile of a simulated cementitious solution prepared with the addition of CO2 loaded AMINE 3.1@P1-2

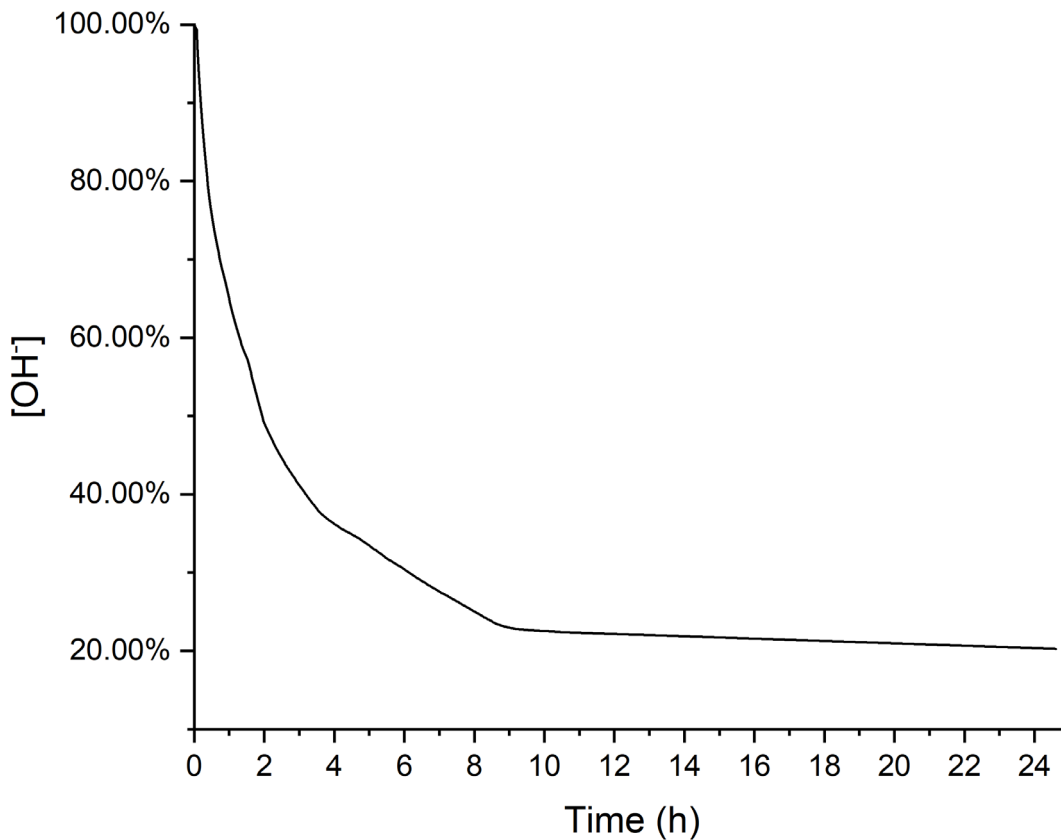


Figure 29: Extrapolated [OH⁻] Consumption profile of a simulated cementitious solution prepared with the addition of CO2 loaded AMINE 3.1@P1-2, to the point of complete solution [OH⁻] consumption

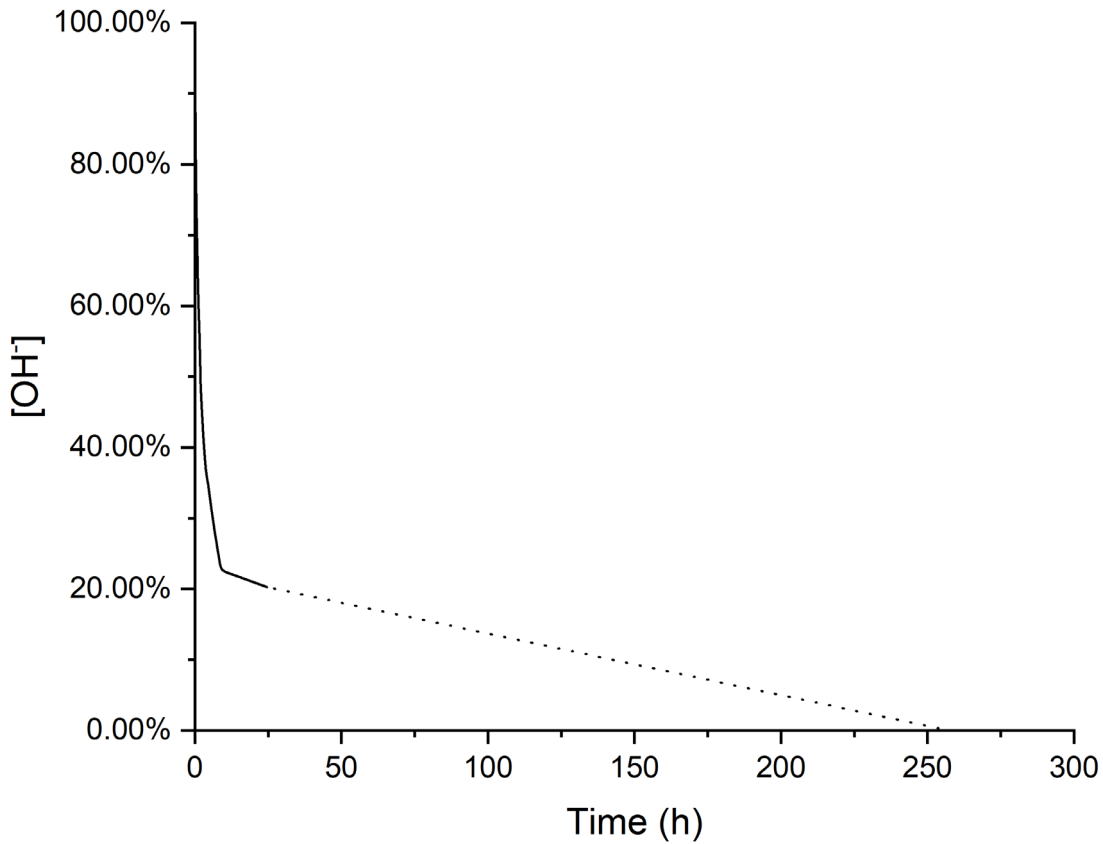
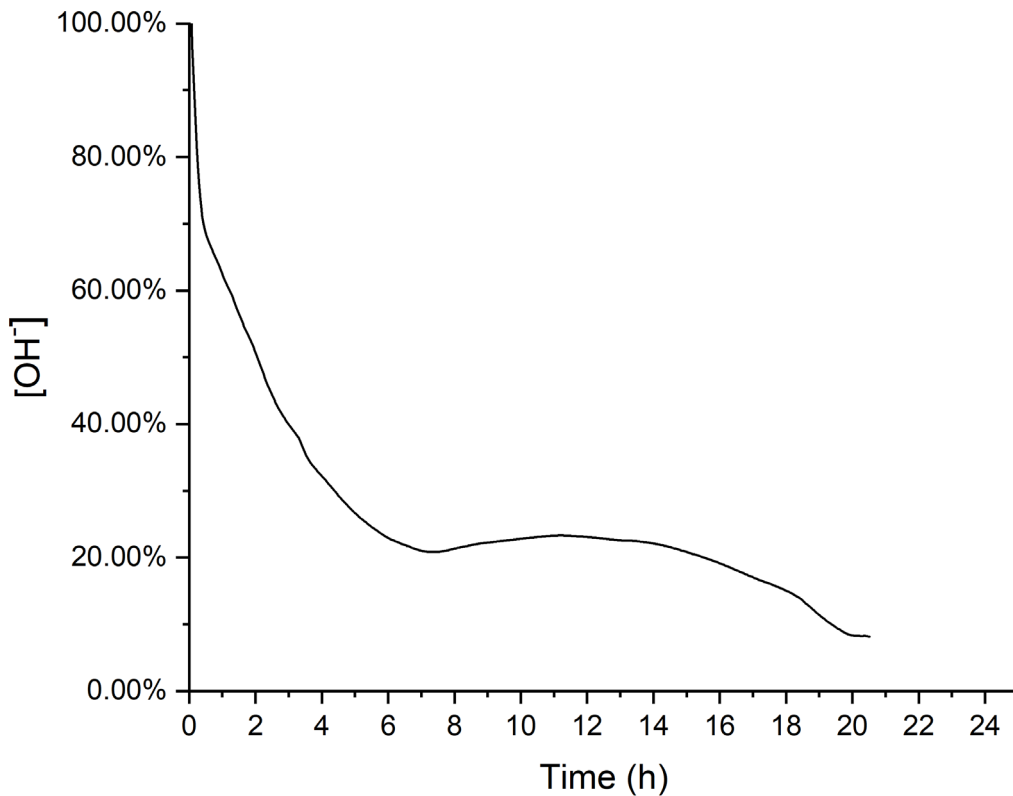


Figure 30: [OH⁻] Consumption profile of a simulated cementitious solution prepared with the addition of CO2 loaded AMINE 3.1@P1-3



AMINE 3.1@P1-2 demonstrated the highest CO₂ adsorption capacity (Table 5), and from the results presented in Figures 31, 32 and 34, also exhibited optimum CO₂ desorption kinetics in an optimised simulated cementitious solution of the three analogues of AMINE 3.1@P1 that were prepared. Simulated solutions with the addition of CO₂ loaded AMINE 3.1@P1-1 (Figure 31) and AMINE 3.1@P1-2 (Figure 32) showed similar profiles of [OH⁻] consumption (hence CO₂ desorption), where release of CO₂ from the respective carriers can be determined to have taken place after 9 hours. AMINE 3.1@P1-1 retains less than 10% of its intrinsic CO₂ adsorption capacity after introduction to the simulated cementitious solution (Figure 31), whereas AMINE 3.1@P1-2 retains over 20 % of previously adsorbed CO₂ in a basic environment. When extrapolated, the [OH⁻] consumption curve of the simulated solution baring CO₂ loaded AMINE 3.1@P1-2 shows that total CO₂ desorption from the carrier proceeds after 257.4 hours (Figure 33), indicating a best-in class amine-grafted carrier material when slow desorption of CO₂ in a simulated cementitious solution is considered.

The [OH⁻] consumption curve of the simulated solution with CO₂ loaded AMINE 3.1@P1-3 (Figure 34) shows a different profile than those in Figures 31 and 32, where insAmine 3d of a single continuous loss of hydroxide, two distinct phases of hydroxide consumption appear to proceed. At the end of measurement, the retained adsorbed CO₂ on AMINE 3.1@P1-3 is less than 10%, hence in terms of adsorption capacity and release rate in a simulated cementitious solution, AMINE 3.1@P1-2 is the optimum alumina supported carrier tested here.

Optimising the amine-grafted carrier to utilise alumina as a support material in place of silica was of interest to improve adsorption capacities, while lowering the rate of CO₂ release in basic environments. AMINE 3.1@P1-2 not only represents a best-in class amine-grafted alumina carrier, but when considering CO₂ release in a simulated cementitious environment, the best-performing amine-grafted carrier examined in Work Package 3. When the [OH⁻] consumption curve of the simulated solution with CO₂ loaded AMINE 3.1@P1-2 is compared to those of identical systems with AMINE 3.1@Si carriers (Figures 19, 20 and 21), AMINE 3.1@P1-2 evidently retains a higher quantity of CO₂ than silica supported carrier materials.

Amine 3.5@P1

In prior study in Work Package 2 (page 18), Amine 3.5@SiO₂ was shown to have improved CO₂ desorption kinetics when compared to the AMINE 3.1@SiO₂, when both prepared in identical procedures where the only differing factor is the nature of the amine that is grafted to the solid support. As AMINE 3.1@P1-2 demonstrated slow CO₂ desorption kinetics, it was theorised that Amine 3.5@P1 would show even slower release rates of CO₂.

Synthesis of Amine 3.5@P1

P1 Powder(1.00 g) was added to a mixture of toluene (100 mL), H₂O (0.25 mL) and Amine 3.5 (4.5 mL), and the reaction mixture was stirred for ~25 minutes at room temperature. The temperature was raised to 70 °C and the reaction was stirred for ~18 hours. On cooling, approximately 2/3 of the reaction supernatant solution was removed via syringe, and the solid product was isolated via centrifugation (15 min, 4500 rpm). The product was washed 3 times

via a cycle of sonication (15 min) in toluene (~20 mL) followed by centrifugation (15 min, 4500 rpm).

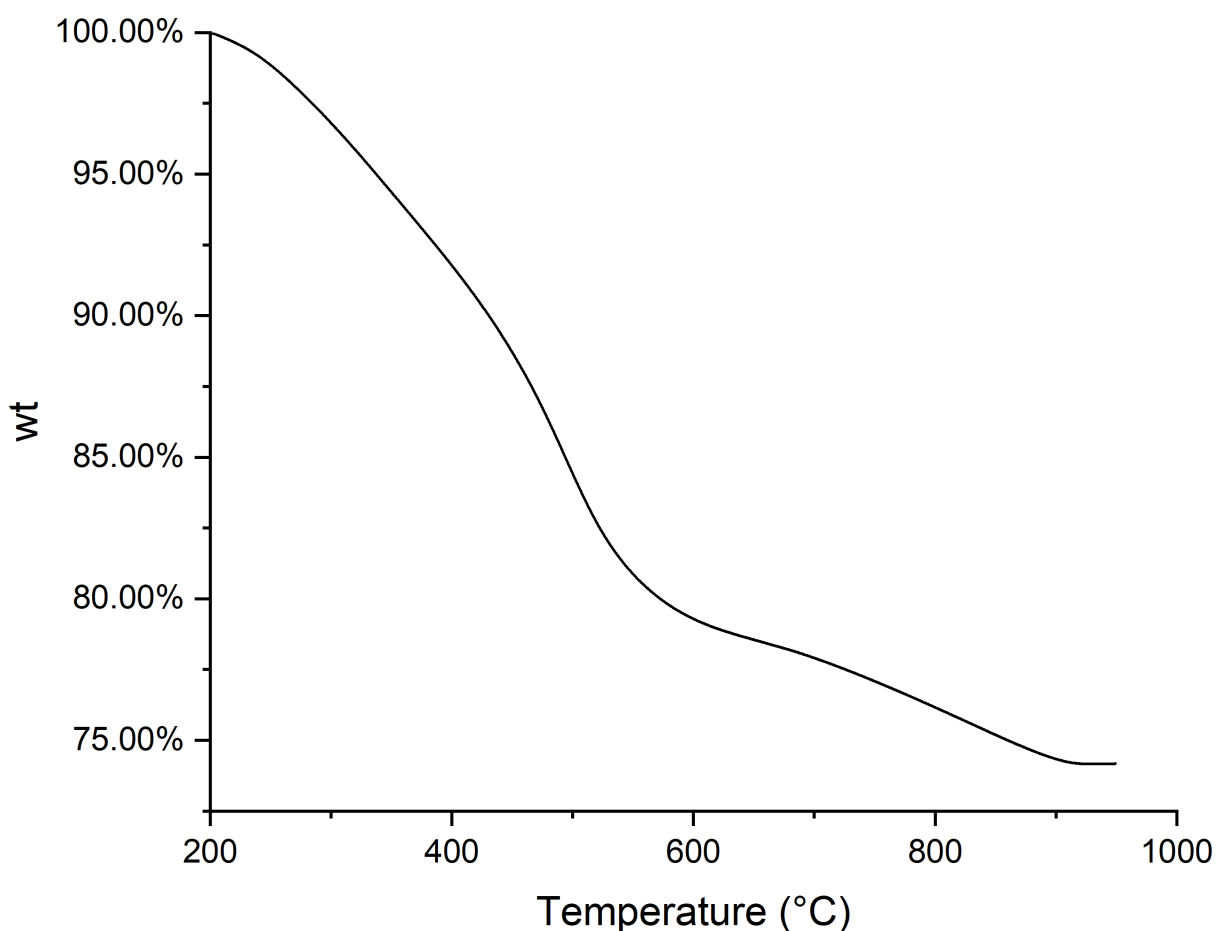
Characterisation – Thermal decomposition

Amine 3.5@P1 was analysed by TGA for thermal decomposition, where the loss in sample mass between the temperature region of 200-800 °C was used to calculate the quantity of Amine 3.5 that was covalently grafted to the surface of the P1 nanoparticles (Table 7).

Table 7: Grafted amine loading on Amine 3.5@P1

Sample	Amine loading / wt%	Amine loading/ mMol g ⁻¹
Amine 3.5@P1	23.84	2.38

Figure 31: Thermal decomposition trace of Amine 3.5@Si



The grafting of Amine 3.5 to P1 nanoparticles resulted in material with a high loading of amine on the solid support. When comparing the 2.38 mMolg⁻¹ loading to that of analogous AMINE 3.1@P1-2 (3.43 mMolg⁻¹, initially the grafting seems less efficient. However as one more of Amine 3.5 contains twice as many amine groups available for the adsorption of CO₂ through

the formation of ammonium-carbamate pairs, then the theoretical CO2 adsorption capacity of Amine 3.5@P1 (prepared according to 4.3.3.1) is higher than AMINE 3.1@P1-2 (prepared according to 4.3.2.1).

Characterisation – High pressure CO2 adsorption

As with the AMINE 3.1@P1 analogues prepared in 4.3.2, the CO2 adsorption capacity of Amine 3.5@P1 was analysed through overnight high pressure adsorption at 70 °C (Table 8).

Table 8: CO2 Adsorption capacity of Amine 3.5@P1 (10 bar CO2, 70 °C, overnight)

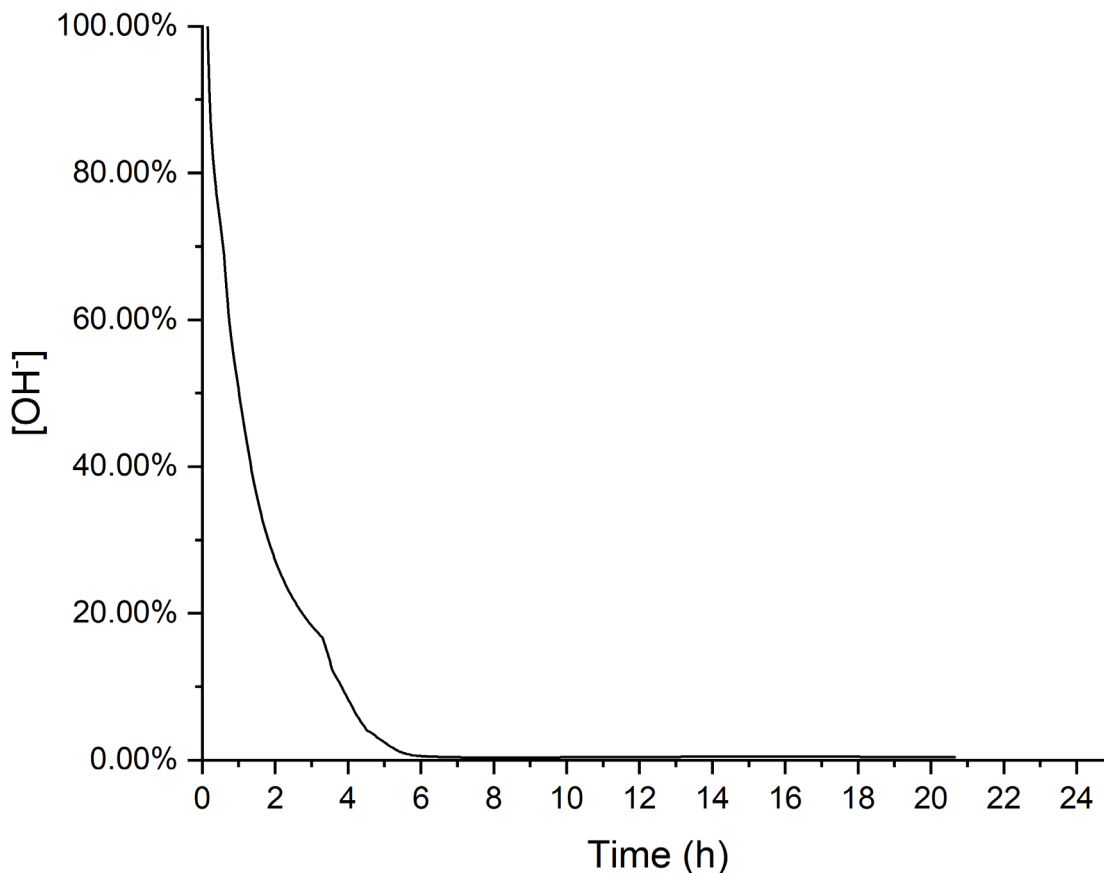
Sample	CO2 capacity (mMol g ⁻¹ / wt %)
Amine 3.5@P1	1.48 / 6.52

Interestingly, when compared to AMINE 3.1@P1-2, the CO2 adsorption capacity of the diamine functionalised carrier is significantly lower than that of the mono-amine functionalised material. Further reaction optimisation may allow for the synthesis of Amine 3.5@P1 carriers with improved CO2 adsorption capacities, however, for the purpose of producing a carrier to investigate for CO2 desorption in a simulated cementitious environment, Amine 3.5@P1 prepared according to the methodology outlined 4.5.3.1 was acceptable.

Characterisation – Simulated solution CO2 desorption

The desorption of CO2 from loaded Amine 3.5@P1 in a simulated cementitious solution was examined, where the hydroxide consumption profile of the basic solution is shown in Figure 36.

Figure 32: [OH⁻] Consumption profile of a simulated cementitious solution prepared with the addition of CO₂ loaded Amine 3.5@P1



The consumption of hydroxide in the simulated cementitious solution with CO₂ loaded Amine 3.5@P1 is a rapid process, indicative of the complete desorption of CO₂ from the carrier shortly after 4 hours. When compared against the hydroxide consumption profiles of the simulated cementitious solutions with CO₂ loaded AMINE 3.1@P1 derivatives, it is evident that grafting the diamine to alumina is not favourable in the synthesis of a carrier that exhibits slow CO₂ desorption in a basic environment. These results are consistent with those detailed in section 4.3.2, where of the amine-grafted silicas examined for CO₂ desorption rate in a basic environment, Amine 3.5@Si exhibited the fastest rate of CO₂ desorption in a simulated cementitious environment.

The grafting of Amine 3.5 to solid supports was outlined in Work Package 2 as a potential way to increase the adsorption capacity of the amine-grafted class of carrier material, through doubling the number of functional groups that are able to form carbamate species per grafted molecule compared to AMINE 3.1. In the case of alumina supported carriers, when the adsorption capacities of AMINE 3.1@P1-2 and Amine 3.5@P1 are considered (Tables 5 and 8), the carrier bearing the monoamine demonstrates a significantly higher adsorption capacity. While research conducted in Work Package 3 has also shown that amine-grafted carriers bearing Amine 3.5 demonstrate significantly faster rates of CO₂ desorption in simulated cementitious environments compared to analogues prepared with grafted AMINE 3.1. From these results, Amine 3.5 grafted materials are evidently not a viable class of CO₂ carrier for use in cement by C4C.

Conclusions and further work

Significant progress has been made in Work Package 3 with regards to both method and carrier development. Prior study in Work Packages 1 and 2 has been built upon, to give a clearer understanding of how CO₂ carriers will perform in cement, through simulated solution experimentation. As it was anticipated the carrier CO₂ desorption under nitrogen even though a good indication is not purely representative of how the same process will proceed in a basic aqueous environment, with differences in desorption rates occurring from loaded carrier materials in these two differing environments.

Preliminary studies into the performance of CO₂ loaded carrier materials in saturated basic solutions were conducted through monitoring solution pH, and using the point of lowest solution pH as the point of complete CO₂ desorption from the carrier. While these experiments gave insight into the nature of CO₂ desorption from different classes of adsorbent carrier, the results could not be used to reliably quantify desorption rate or the amount of CO₂ released from the carrier over a 24 hour duration in the specific environment. While not in the initial remit of these tests, interesting observations in overall pH decrease of systems with different suspended carrier material could be used to determine the relative amount of leaching of impregnated or grafted amine to the basic solution. AMINE 1(50%)@PQ-Si (M25) exhibited the slowest loss of CO₂ in this testing regime.

Low concentration Ca(OH)₂ experiments detailed an early-stage hydration system whereby the performance of several carriers could be evaluated according to their drop-off time until all Ca(OH)₂ was consumed. Again, AMINE 1(50%)@PQ-Si (M25) exhibited the slowest loss of CO₂ in this testing regime.

Further method development on simulated solution testing allowed for the direct quantification of CO₂ release from carriers, in solutions designed to represent the basicity of 7Amine 3.4y old hydrated cement. The quantity of CO₂ added to the systems via loaded carrier was equal to the concentration of Ca(OH)₂ in these solutions. Therefore, since CO₂ reacts with Ca(OH)₂ in a 1:1 reaction, through measuring pH and subsequently calculating the concentration of hydroxide ions in the solution, the consumed hydroxide could be directly related to CO₂ released from the carriers. A wide range of carrier materials previously identified as potential candidates for use by C4C in Work Packages 1 and 2 were examined for CO₂ release in a simulated cementitious solution. Amine-impregnated Polymer 1-AMINE 3 carriers proved unsuitable for measuring CO₂ release in a simulated cementitious solution via this method, owing to assumed polymer decomposition in aqueous base leading to the release of AMINE 3 to the solution. As AMINE 3 is a strong base, its release caused dramatic fluctuations in solution pH, resulting in the calculated [OH⁻] evolution traces shown in Figure 23 being highly sporadic, and no conclusions could be drawn from this data. There was a compatibility between amine-grafted materials and the simulated cementitious solution that allowed for the calculation of solution [OH⁻], and as a result, the nature of CO₂ release from these materials. There were differences in the profiles of CO₂ desorption from different classes of AMINE 3.1@Si carriers. AMINE 3.1@Si_0.30 and AMINE 3.1@Si_0.35 showed a much faster initial

rate of CO₂ release than AMINE 3.1@Si_{0.45}, however, after a 24 hour measurement period the initial hydroxide quantity had been mostly consumed in solutions containing all three of these carriers (Figures 19, 20 and 21). Investigation into the use of AMINE 3.1@Si as adsorbed carriers for use in cement by C4C is hence now no longer of interest. Interestingly, Amine 3.5@Si, a carrier formulation known to exhibit excellent CO₂ retention capabilities under a nitrogen atmosphere (Table 3), showed the fastest rate of CO₂ release from the amine-grafted silica carriers examined in a simulated cementitious solution, and also no longer presented itself as a viable carrier for use in cement by C4C. The CO₂ retention capabilities of amine-impregnated silica carriers followed a predicted trend, where those with high loading capacities of high molecular weight amine adsorbent demonstrated the most labile consumption of simulated cementitious solution hydroxide concentration. AMINE 1(50%)@PQ-Si (M25) exhibited the slowest consumption of simulated solution hydroxide of all the carriers examined, which can be attributed to slow release of CO₂ from the carrier material. Of the previously studied carriers tested for the release rate of CO₂ in a simulated cementitious solution, **AMINE 1(50%)@PQ-Si (M25)** is the most clear candidate for further study by C4C.

Preliminary investigation into the performance of amine-grafted carriers utilising alternative support materials was also conducted as part of WP-3.2, specifically, carriers using alumina as a support. Preliminary investigation into carrier CO₂ adsorption capacity, and CO₂ release rates under a nitrogen atmosphere highlighted AMINE 3.1@P1-2 (prepared according to the procedure detailed in 4.5.2.1) as a high capacity carrier with strong CO₂ retention capabilities under N₂. However, previous study conducted in Work Package 3 had made it apparent that a slow release CO₂ carrier under nitrogen would not necessarily translate to a carrier that exhibits similar desorption kinetics in a simulated cementitious solution. Using the same methodology as described in 4.1 for carrier performance evaluation in a simulated cementitious environment, AMINE 3.1@P1-2 was shown to demonstrate a moderate release rate of CO₂, with over 20 % of initially adsorbed CO₂ remaining on the carrier after a 24 hour monitoring period (Figure 32). The near constant hydroxide concentration of the simulated solution bearing this loaded carrier after 10 hours (Figure 32) indicates that a proportion of the CO₂ adsorbed by this carrier is strongly bound and resistant to base mediated desorption in a simulated 7Amine 3.4y old cementitious solution environment. These preliminary results are promising, and highlight AMINE 3.1@P1 as viable carrier for further development by C4C.

Both AMINE 1(50%)@PQ-Si (M25) and AMINE 3.1@P1 have demonstrated CO₂ desorption kinetics in simulated cementitious solutions in WP3 to allow for further experimentation on these carriers to proceed in further Work Packages. AMINE 1(50%)@PQ-Si (M25) represents a best-in class amine-impregnated silica carrier, exhibiting complete CO₂ desorption over a duration of 73.4 hours, whereas AMINE 3.1@P1-2 demonstrated optimum CO₂ desorption kinetics of all carrier materials examined thus far. Complete CO₂ desorption from AMINE 3.1@P1-2 in a simulated cementitious solution environment proceeded after a long duration of 257.4 hours, a highly promising result for further carrier development.

If you need a version of this document in a more accessible format, please email alt.formats@energysecurity.gov.uk. Please tell us what format you need. It will help us if you say what assistive technology you use.